R and D CENTER LABORATORY

TECHNICAL REPORT

No. 13042

# Hypergolic Combustion Demonstration in a Reciprocating Internal Combustion Engine

Contract Number DAAE07-81-C4121

May 1984

by D. H. Scharnweber
Eaton Corporation
Engineering & Research Center
26201 Northwestern Highway
P.O. Box 766
Southfield, Michigan 48037
Eaton Technical Report No. 84033





U.S. ARMY TANK-AUTOMOTIVE COMMAND
RESEARCH AND DEVELOPMENT CENTER
Warren, Michigan 48090

## NOTICES

This report is not to be construed as an official Department of the Army position.

Mention of any trade names or manufacturers in this report shall not be construed as an official endorsement or approval of such products or companies by the U. S. Government.

Destroy this report when it is no longer needed. Do not return it to the originator

# REPORT DOCUMENTATION PAGE

| | |
|---|---|
| 1a. REPORT SECURITY CLASSIFICATION<br>Unclassified | 1b. RESTRICTIVE MARKINGS |
| 2a. SECURITY CLASSIFICATION AUTHORITY | 3. DISTRIBUTION/AVAILABILITY OF REPORT<br>Approved for Public Release<br>Distribution Unlimited |
| 2b. DECLASSIFICATION/DOWNGRADING SCHEDULE | |
| 4. PERFORMING ORGANIZATION REPORT NUMBER(S)<br>ERC Technical Report No. 84033 | 5. MONITORING ORGANIZATION REPORT NUMBER(S)<br>13042 |
| 6a. NAME OF PERFORMING ORGANIZATION<br>Eaton Corporation<br>Engineering & Research Center<br>6b. OFFICE SYMBOL (If applicable) | 7a. NAME OF MONITORING ORGANIZATION<br>US Army Tank-Automotive Command<br>AMSTA-RGRD |
| 6c. ADDRESS (City, State, and ZIP Code)<br>Southfield, Michigan 48037 | 7b. ADDRESS (City, State, and ZIP Code)<br>Warren, Michigan 48090 |
| 8a. NAME OF FUNDING/SPONSORING ORGANIZATION<br>8b. OFFICE SYMBOL (If applicable) | 9. PROCUREMENT INSTRUMENT IDENTIFICATION NUMBER<br>DAAE07-81-C4121 |
| 8c. ADDRESS (City, State, and ZIP Code) | 10. SOURCE OF FUNDING NUMBERS<br>PROGRAM ELEMENT NO. / PROJECT NO. / TASK NO. / WORK UNIT ACCESSION NO. |
| 11. TITLE (Include Security Classification) Hypergolic Combustion Demonstration in a Reciprocating Internal Combustion Engine | |
| 12. PERSONAL AUTHOR(S) Scharnweber, David H. | |
| 13a. TYPE OF REPORT Final<br>13b. TIME COVERED FROM 81 Sep TO 84 May | 14. DATE OF REPORT (Year, Month, Day) 84 May<br>15. PAGE COUNT 50 |
| 16. SUPPLEMENTARY NOTATION | |

| 17. COSATI CODES | | | 18. SUBJECT TERMS (Continue on reverse if necessary and identify by block number) |
|---|---|---|---|
| FIELD | GROUP | SUB-GROUP | Hypergolic Combustion, High-Temperature Fuel Injection, Phyrophoric Combustion, Ignition Delay Reduction, Preheated Fuel, |
| | | | |
| | | | |

19. ABSTRACT (Continue on reverse if necessary and identify by block number)

The theory of hypergolic combustion was experimentally verified in a reciprocating internal combustion engine by preheating the fuel to near 1000°F before direct high pressure injection into the combustion chamber. Dramatic reductions in ignition delay and exhaust smoke were observed. The potential for combustion rate control and a major improvement in engine power density were also demonstrated. Multi-fuel operation was addressed. Originator Supplied Keywords include:

| | |
|---|---|
| 20. DISTRIBUTION/AVAILABILITY OF ABSTRACT<br>☒ UNCLASSIFIED/UNLIMITED ☐ SAME AS RPT. ☐ DTIC USERS | 21. ABSTRACT SECURITY CLASSIFICATION<br>Unclassified |
| 22a. NAME OF RESPONSIBLE INDIVIDUAL<br>Constantine Panagos | 22b. TELEPHONE (Include Area Code) (313)574-6147<br>22c. OFFICE SYMBOL AMSTA-RGRD |

DD FORM 1473, 84 MAR 83 APR edition may be used until exhausted. All other editions are obsolete.

## SUMMARY

The theory of hypergolic combustion by means of preheating the fuel to near 1,000°F was experimentally verified on a single-cylinder diesel engine using diesel-like distillate fuels. Ignition delay was reduced by 80%, which offers the promise of combustion rate control with the development of fuel injection rate control. Exhaust smoke opacity reductions of 60-95% were typical. The potential for a major improvement in engine power density was demonstrated by an observed 25% reduction in peak cylinder pressure for the same indicated mean effective pressure and up to a 90% reduction in rate of cylinder pressure rise. Virtual elimination of the conventional initial heat release spike was observed and may make a major reduction in oxides of nitrogen emissions.

Alternate fuel tests with methanol and isooctane preheated to 1,300°F and 1,000°F, respectively, produced erratic combustion insufficient for normal documentation. Further hypergolic combustion investigation with alternate fuels is warranted.

High-temperature fuel deposits that in most cases completely plugged the fuel heating system were the major problem. These deposits limited the typical maximum effective hot fuel test duration to 35 minutes.

TABLE OF CONTENTS

## LIST OF ILLUSTRATIONS

LIST OF TABLES

## 1.0. INTRODUCTION

1.1. This final Technical Report, prepared by the Engineering & Research Center (ERC) of Eaton Corporation for the U.S. Army Tank-Automotive Command under Contract DAAE07-81-C4121, describes the effort to demonstrate the existence of hypergolic combustion in a reciprocating internal combustion engine by means of supercritical heating of the fuel before direct injection into the cylinder. Hypergolic combustion, with its resulting dramatic reduction in ignition delay and elimination of the fuel droplet aspect of conventional diesel diffusion-limited combustion, could contribute to the overall mission of TACOM by providing an engine with improved power density, fuel tolerance, smoke signature, noise, and emissions.

1.2. In 1977, Dr. L. O. Hoppie(1)(2)(3) of Eaton ERC developed a mathematical model to predict theoretical ignition delay as a function of initial fuel and air temperature. This model predicts that the ignition delay of virtually any fuel starts to decrease rapidly at 800°F fuel temperature, and will be reduced to negligible values above 1,100°F fuel temperature. A complete definition of this model and a review of heated fuel efforts by other researchers is presented in SAE Paper 820356 written by Dr. Hoppie and reprinted with permission of SAE in Appendix A. This theoretical effort was followed by an experiment also carried out at Eaton in which preheated diesel fuel was injected into air at atmospheric temperature and pressure. As expected, room temperature fuel ignited upon contact with a bunsen burner and burned with an orange sooty flame. However, fuel preheated to near 1,000°F ignited without coming in contact with the burner and burned with a completely blue flame. These analytical and experimental efforts were the basis for the experimental engine effort with preheated fuel conducted under this contract.

## 2.0. OBJECTIVES

The objectives of this contract were to demonstrate hypergolic combustion and determine its benefits in a reciprocating internal combustion engine by preheating the fuel.

## 3.0. CONCLUSIONS

Hypergolic combustion can be achieved in a reciprocating internal combustion engine by preheating the fuel.

The dramatic reduction in ignition delay, in conjunction with fuel injection rate and duration control, provides much better combustion control. It should be possible to design an engine based on hypergolic combustion to provide a significant increase in power density and thermal efficiency for a reduced maximum cycle pressure and decreased oxides of nitrogen emissions. The droplet aspect of conventional

diesel diffusion-limited combustion is eliminated when fuels are preheated to the hypergolic region with a resultant dramatic reduction in exhaust smoke emissions.

Hypergolic combustion should provide increased fuel tolerance; however, additional investigation in the multifuel area is needed. The formation of detrimental high-temperature fuel deposits in the fuel heater and problems associated with handling hot fuel must be addressed if hypergolic combustion is to be reduced to practice.

## 4.0. RECOMMENDATIONS

The demonstrated existence and potential benefits of hypergolic combustion warrant further investigations, including indepth combustion research. An investigation focused on obtaining a full understanding of the formation of high-temperature fuel deposits should be conducted so that potential solutions can be identified. Practical means of preheating the fuel should be conceived and experimentally assessed. Also, the full implications of combustion control should be analytically and experimentally investigated.

## 5.0. DISCUSSION

### 5.1. Background

Conventional diesel engines have droplet-type diffusion-limited combustion involving atomization, vaporization, mixing, precombustion reactions, ignition, and combustion. The time between the start of fuel injection into the combustion chamber and the start of combustion pressure rise is called the ignition delay and is an important parameter affecting fuel specifications and engine emissions, noise, and stress considerations. Ignition delay is the sum of physical delay and chemical delay. Physical delay involves the time for spray atomization, vaporization, and mixing. Chemical delay involves the time for preflame reactions to occur. These reactions produce intermediate species in an activated state which are needed for ignition and subsequent combustion. With droplet-type, diffusion-limited combustion, pyrolytic decomposition of the fuel results in carbon particulate which is the cause of the black exhaust smoke signature characteristic of diesel engines. If the ignition delay could be reduced to negligibly small values, the rate of combustion could be totally controlled by the rate of fuel injection and mixing. This, in turn, would lead to higher efficiency and specific power at reduced emissions.

For the purpose of investigating hypergolic combustion in this experimental project, the fuel was preheated to temperatures as high as 1,200$^{o}$F at pressures between 1,500-3,000 PSI. In Figure 5-1, this experimental hypergolic region is shown on an enthalpy-temperature diagram for petroleum fractions with a 500$^{o}$F mean average boiling point(4), together with the heating path for fuel at the 2,000

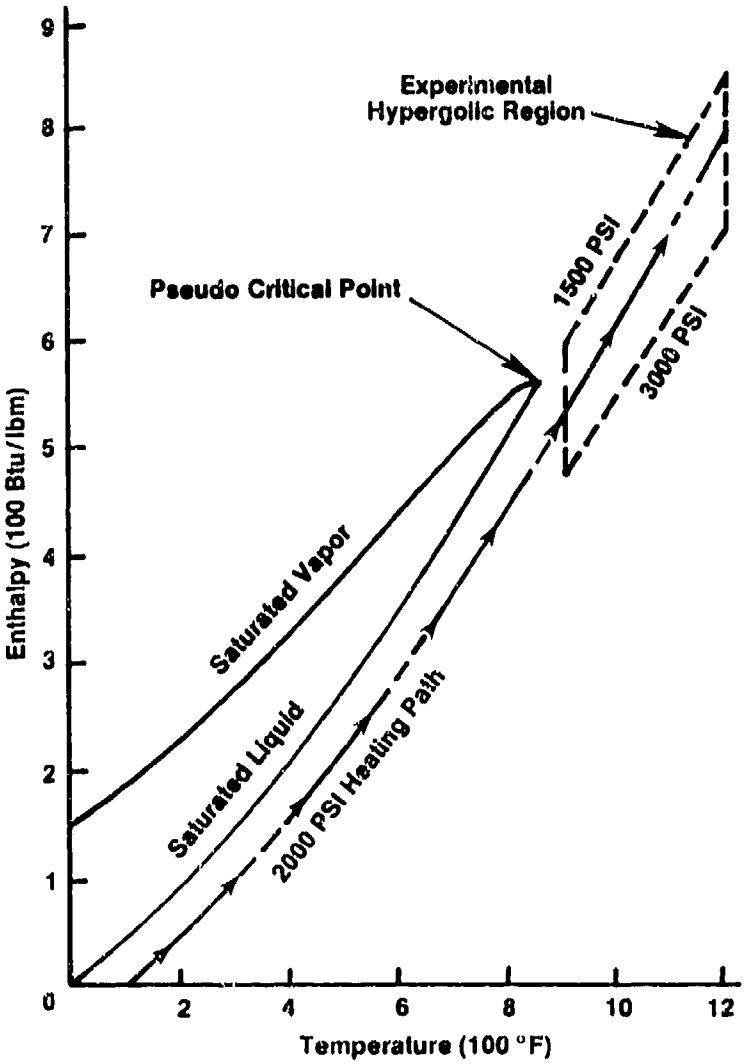


**Figure 5-1. Enthalpy vs. Temperature for Petroleum Fractions with 500°F Mean Average Boiling Point**

PSI pressure commonly used during this test program. The fuel undergoes a continuous transition from the liquid to the supercritical fluid phase without boiling as it is heated through the critical temperature and is highly compressible in the experimental hypergolic region. Therefore, droplet-type diffusion limited combustion is eliminated and fuel-air mixing is the only remaining physical delay factor. Furthermore, when fuel is preheated to the hypergolic region, a significant amount of the fuel is in an activated radical state so that the chemical delay is virtually eliminated.

## 5.2. Test Engine

The test engine was a commercially available Deutz Model F1L411D naturally aspirated direct injection single-cylinder diesel engine. This engine has a 3.62 in. bore, 4.13 in. stroke, 42.5 $in^3$ displacement, 17.0 to 1 nominal compression ratio, and a rated power of 11.5 bhp at 2,500 RPM (118 PSI IMEP). This engine came from existing Eaton inventory and was selected because of its previous reliable performance on R&D projects and its good adaptability to modifications required to incorporate the experimental high-temperature fuel injector. The combustion chamber, porting, valves, and valve timing were not altered during this test program. Photographs of the test engine with the experimental high-temperature fuel injection system are shown in Figures 5-2 and 5-3.

## 5.3. Experimental Fuel Injection System

5.3.1. System Concept. The purpose of the experimental high-temperature fuel injection system was to function as a research tool to permit demonstration of the hypergolic combustion phenomenon in an actual engine. It was designed solely for this purpose and was not intended to reflect any attempt to address practical application considerations. A common rail type fuel system concept was selected because of the need to isolate precision pumping components from high-temperature fuel, and because the greatly increased compressibility of fuel heated to the supercritical fluid region prevents using the fuel as a hydraulic actuation liquid. The system was designed for a maximum 1,200°F fuel temperature, 3,000 PSI fuel supply pressure, and 2,500 RPM engine speed. A schematic drawing of the experimental high-temperature fuel injection system is shown in Figure 5-4. Details of the fuel system are discussed subsequently in this section.

### 5.3.2. Fuel Injector Design

5.3.2.1. Level 1 injector design. A cross-sectional drawing of the Level 1 experimental fuel injector design is shown in Figure 5-5. This design is based on a differential area actuation piston assembly that is driven by a hydraulic circuit separate from the hot fuel supply. The hydraulic actuation pulse lifts the actuation piston and removes the main spring load from the hot fuel needle, allowing hot fuel supply pressure, acting on the hot needle differential area, to lift the hot needle to the maximum lift stop. The main spring returns the hot needle to the nozzle seat when the hydraulic actuation pulse is completed. The actuation valve controls the

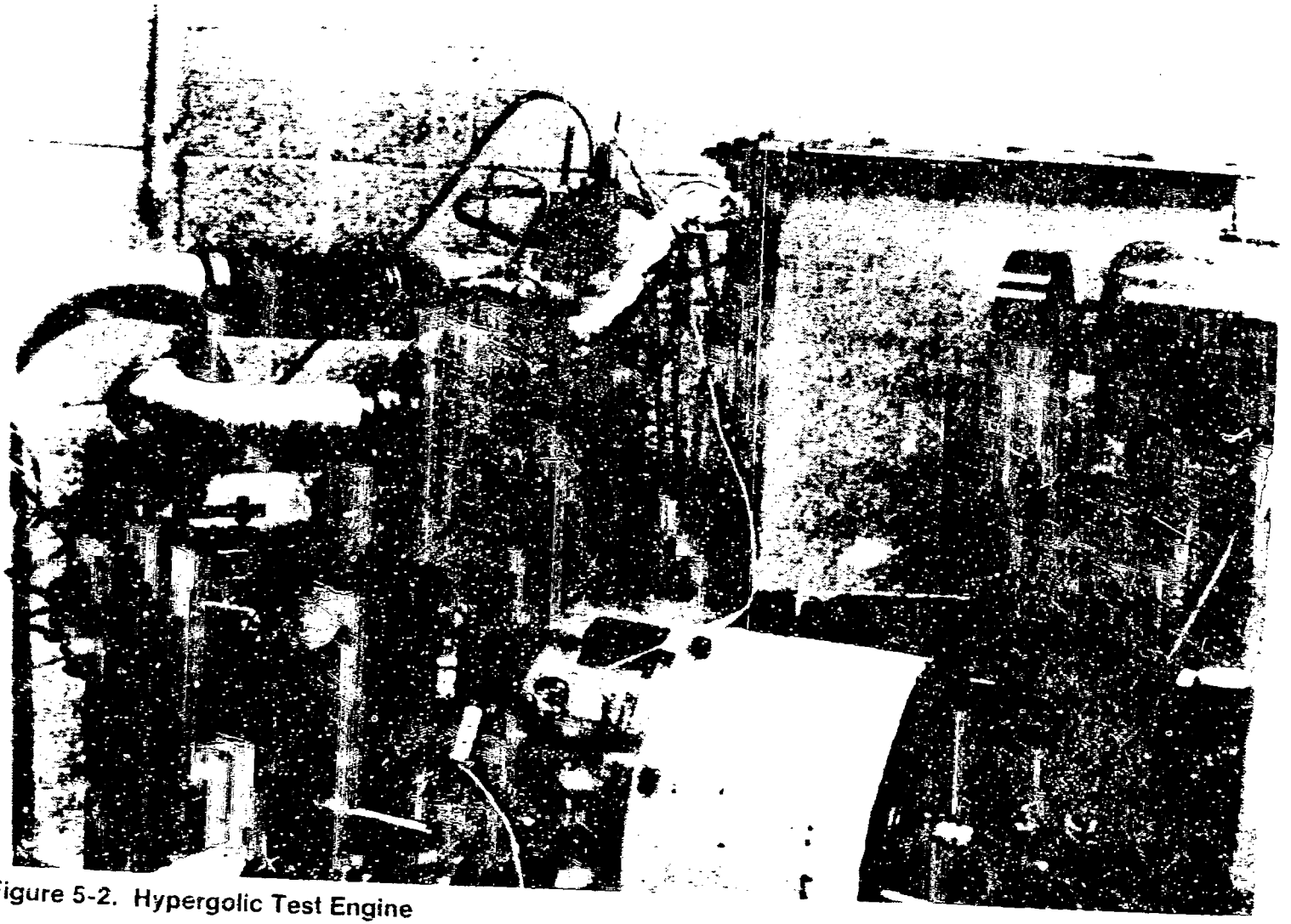

Figure 5-2. Hypergolic Test Engine

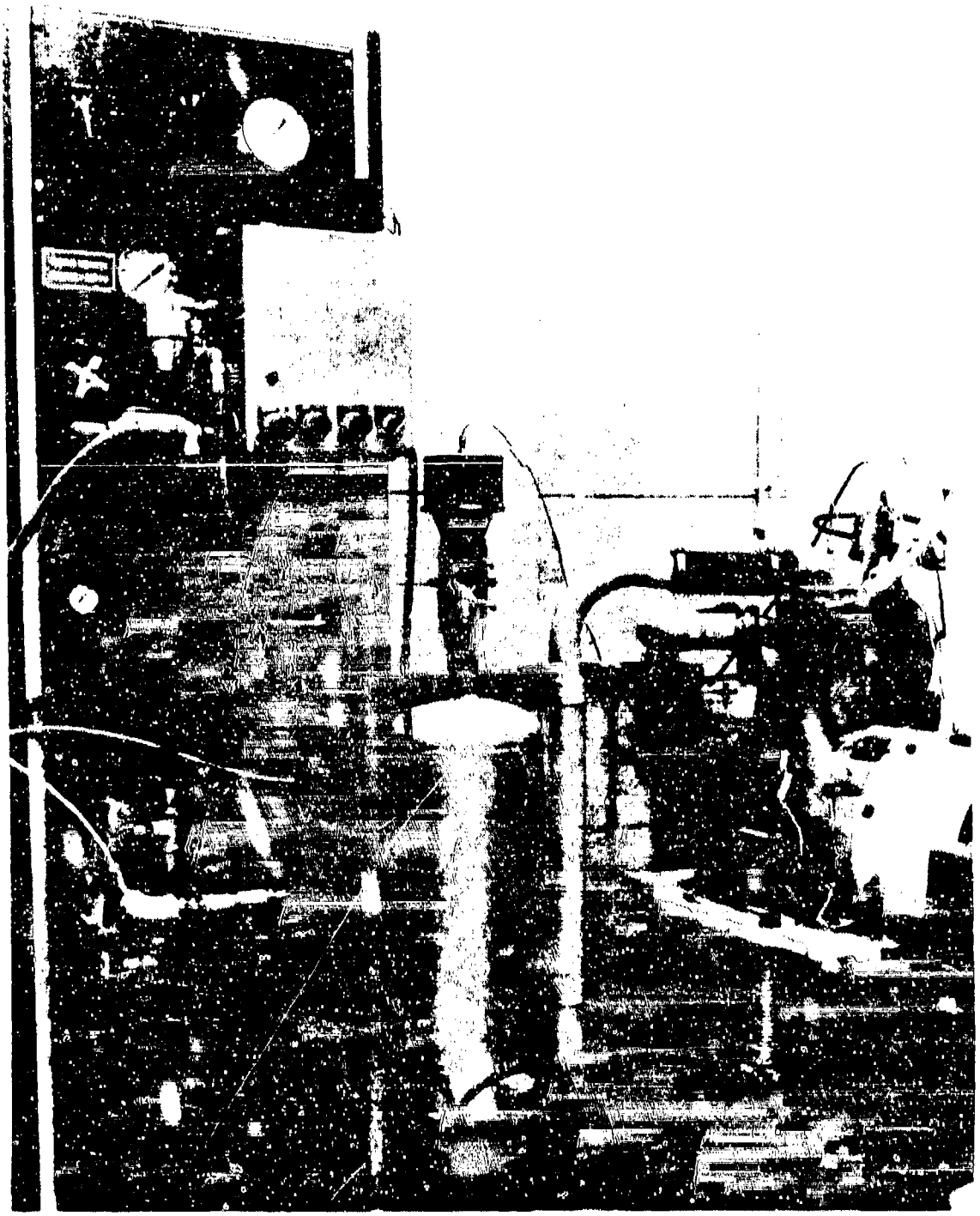

**Figure 5-3. Hypergolic Test Engine**

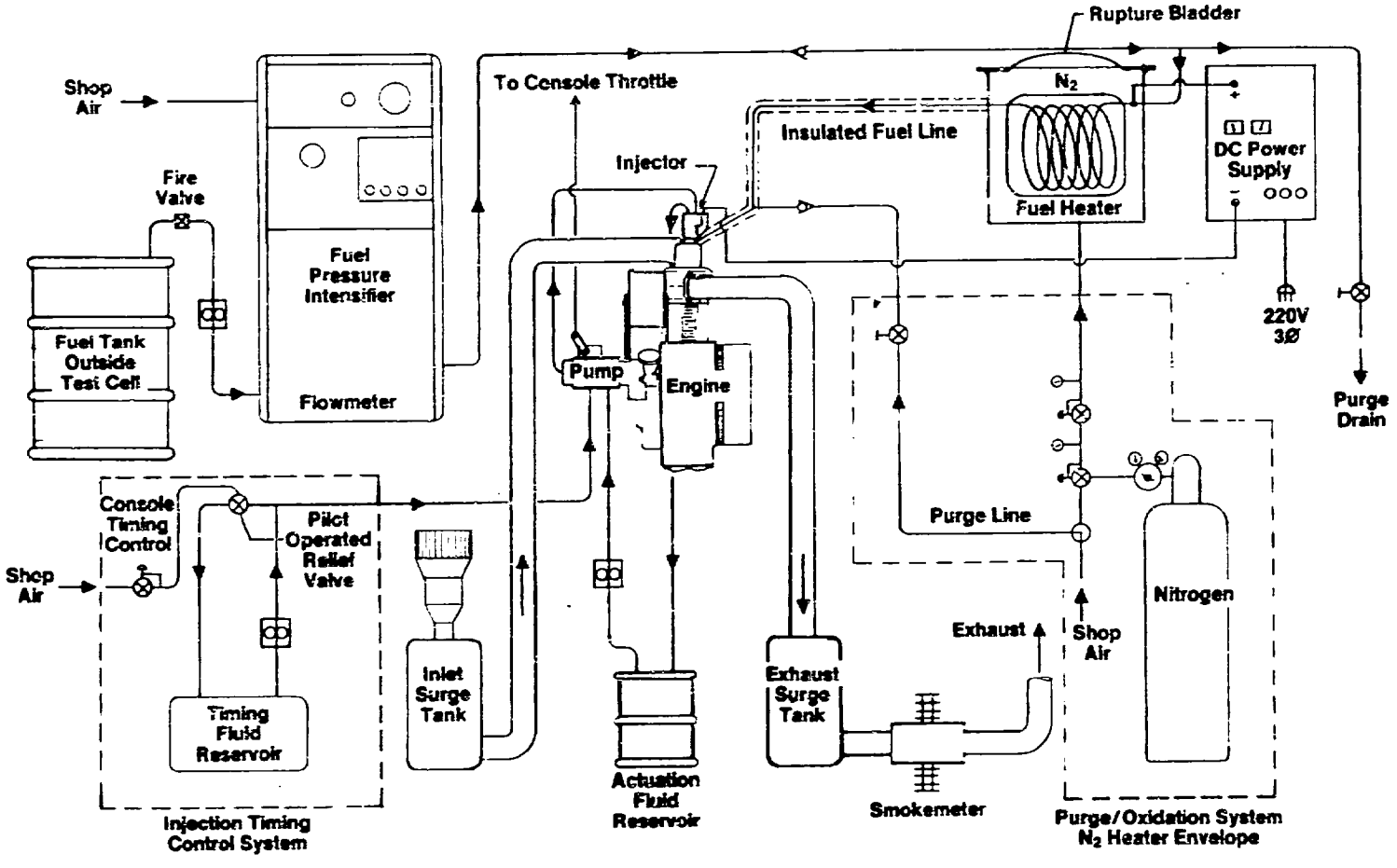


**Figure 5-4. Experimental High Temperature Fuel Injection System Schematic**

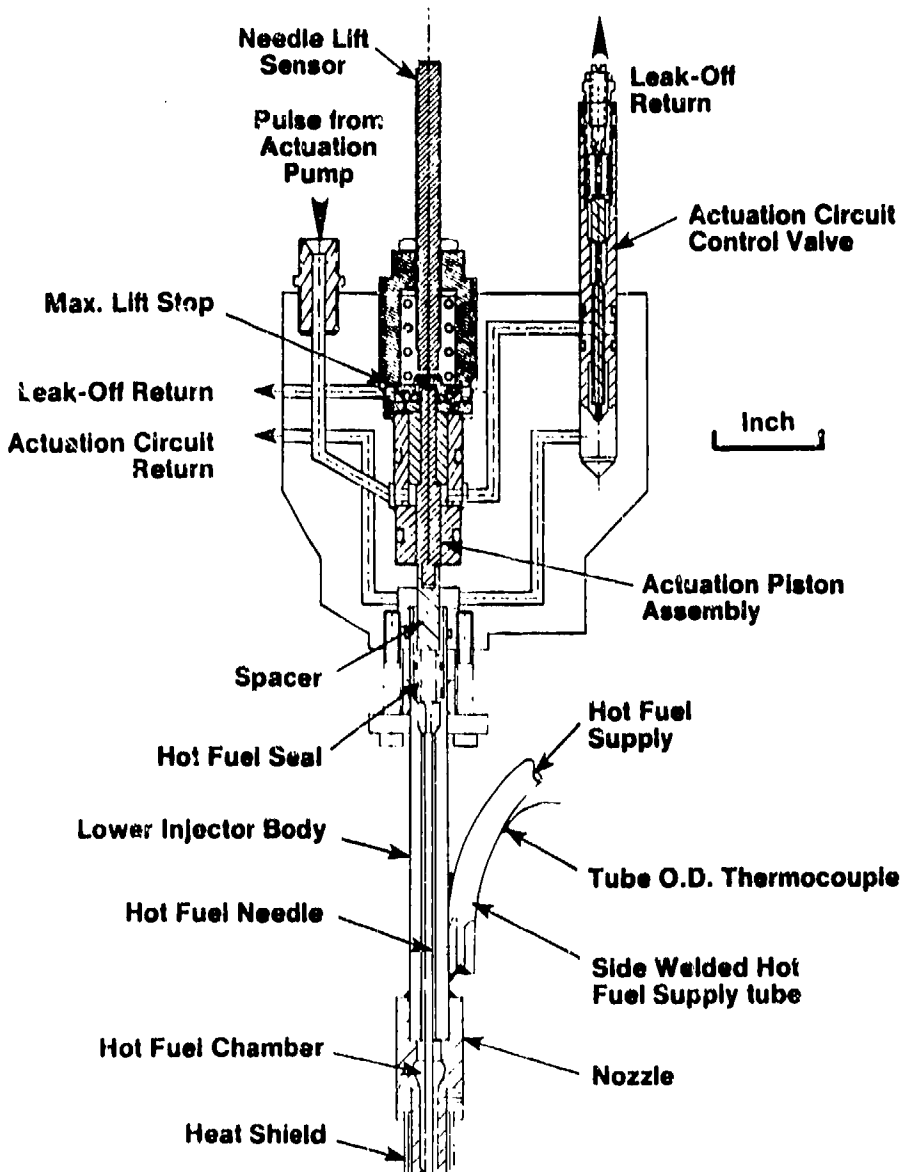


**Figure 5-5. Level 1 Experimental Fuel Injector Design**

actuation circuit pressure, wave dynamics, and discharges the actuation liquid volume into the return circuit. The actuation return liquid was routed over the hot fuel seal sleeve to provide limited cooling. The hot fuel seal consists of a close fit between the hot needle seal land and hot needle seal sleeve. The seal sleeves were OEM material, and the installation threads were secured with a zirconia ceramic cement. The seal sleeve-to-needle diametrial clearance was maintained in the 0.00010 to 0.00020 inch range to allow for differential thermal expansion. The seal sleeve interface was treated with a high-temperature molybdenum lubricant. The high location of the hot fuel seal over the hot fuel inlet was intended to provide fuel column insulation. The sac tip type nozzle body was a modified OEM unit with four 0.0105-inch diameter orifices at the same OEM angle orientation. The maximum lift was adjustable between 0.005 to 0.035 inch. Hot needle lift was measured with a proximity sensor targeted on the main spring spindle. A shim stack and double air gap stainless steel heat shield were used to reduce nozzle body heat loss to the aluminum cylinder head.

5.3.2.2. Level 1 injector performance. This design configuration was used during the bench test development of the hydraulic actuation circuit and initial shakedown testing of the engine with hot fuel. The hydraulic actuation circuit performed well at hot fuel supply temperatures in the 800-1,000°F range. However, sticking of the hot needle prevented obtaining substantive hot fuel performance data. The hot needle sticking was caused by excessive thermal distortion of the lower injector body. The gradual retardation and eventual sticking of the hot needle caused separation between the actuation piston and hot needle and prevented meaningful measurement of needle lift. These problems lead to the Level 2 injector design.

5.3.2.3. Level 2 injector design. A cross-sectional drawing of the Level 2 experimental fuel injector design is shown in Figure 5-6. Thermal distortion of the lower injector body was greatly reduced by incorporating a symmetrical flange to introduce the hot fuel supply to the injector, and by reducing the constrained length between the mounting bracket and the mounting seat. Furthermore, the actuation piston and hot needle were mechanically connected with an articulated link. This link ensured accurate needle lift measurement and increased needle lift rate by allowing the actuation piston lift force to assist lifting the hot needle. Replacement seal sleeves were made from 316 and 17-7PH stainless steels. The hydraulic actuation circuit, nozzle tip configuration, and nozzle heat shield remained the same as the Level 1 design.

5.3.2.4. Level 2 injector performance. This injector design was used during all tests that produced substantive high-temperature fuel engine test data. The main disadvantage of this design was that high-temperature fuel deposits were difficult to remove from the welded lower injector assembly.

5.3.2.5. Level 3 injector design. A cross-sectional drawing of the Level 3 experimental fuel injector design is shown in Figure 5-7. The lower injector section was redesigned to provide easy disassembly for cleaning, to reduce hot fuel dead volume, and to reduce heat flux to the hydraulic head. A divorced hot fuel

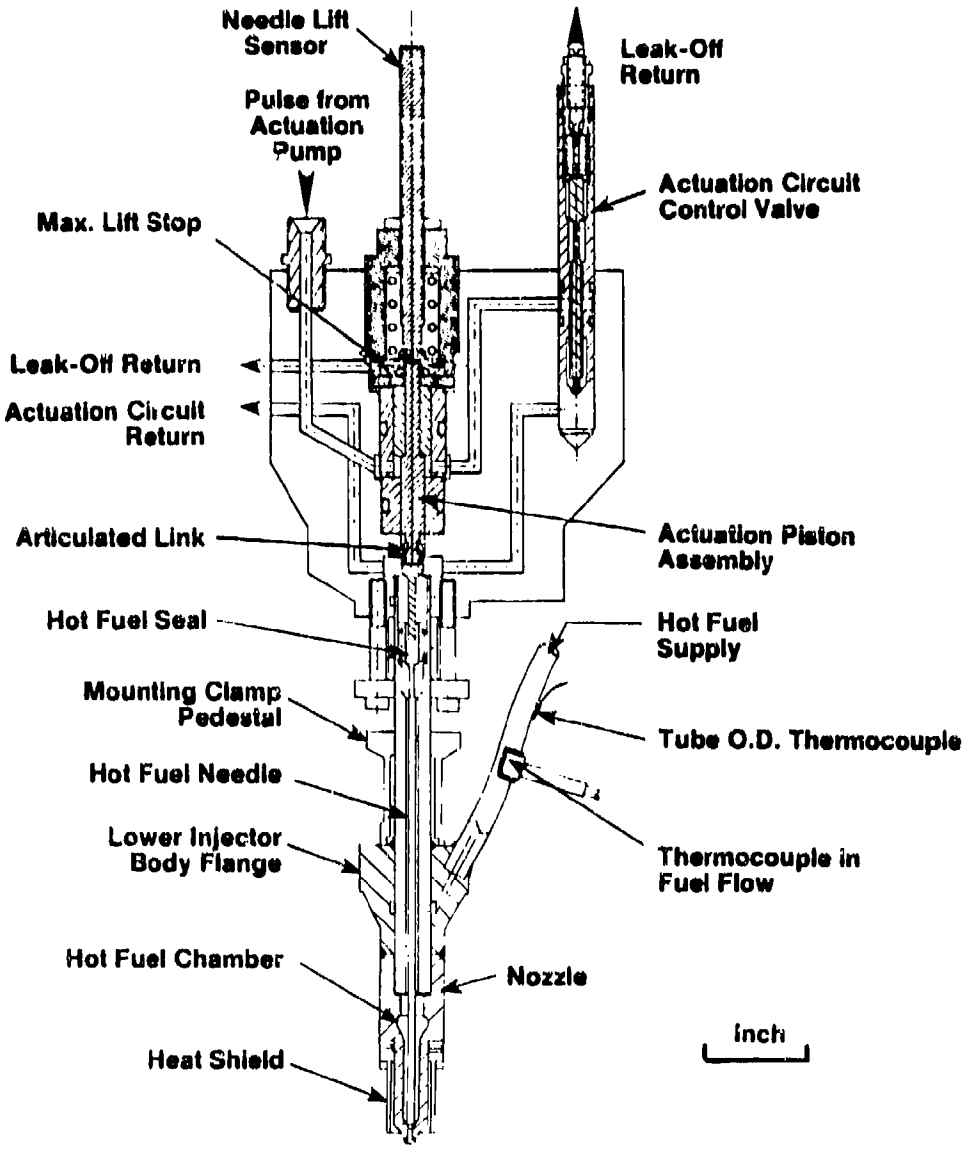


**Figure 5-6. Level 2 Experimental Fuel Injector Design**

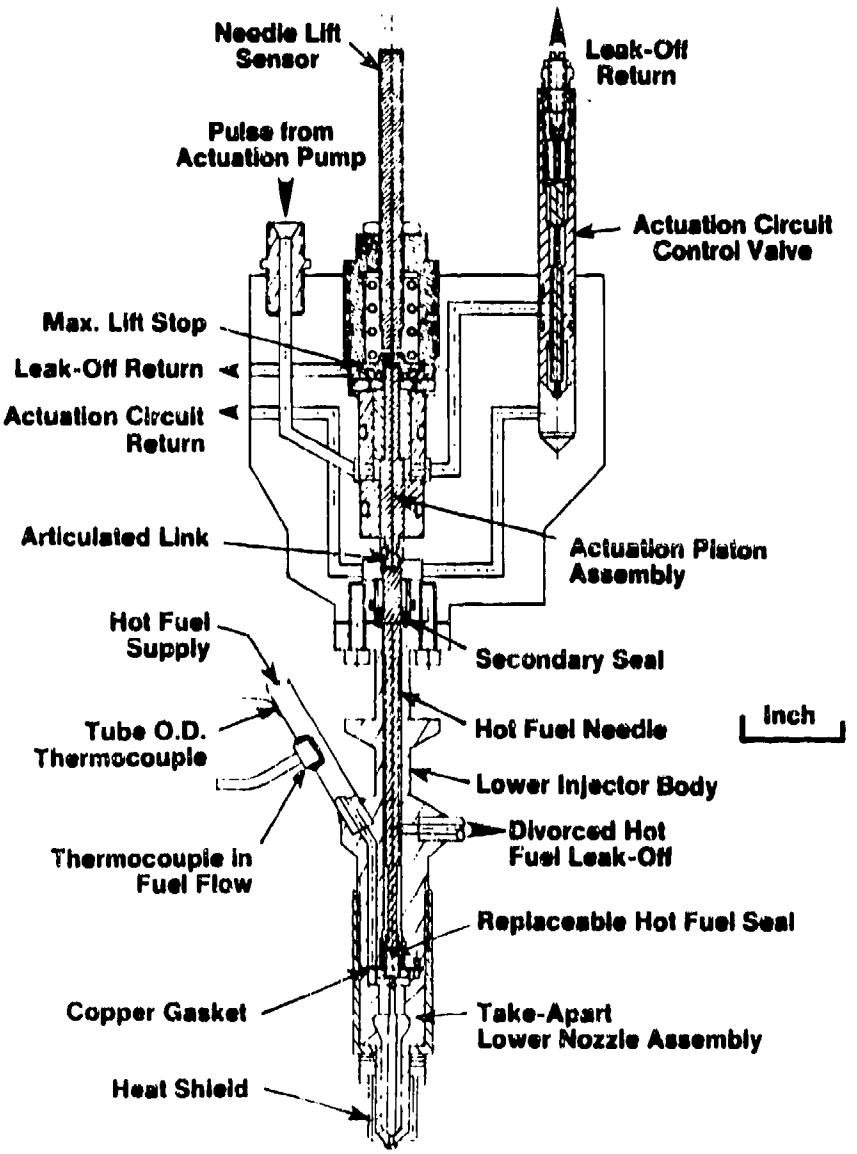


Figure 5-7. Level 3 Experimental Fuel Injector Design

leak-off circuit together with provisions for easy replacement of hot fuel seal sleeves and nozzle bodies were also incorporated. The hydraulic actuation circuit and the nozzle heat shield remained the same as in the Level 1 and 2 designs.

5.3.2.6. Level 3 injector performance. This injector design was used late in the program during the alternate fuel tests. Most of the problems were fuels/combustion related. Injector problems were mainly galling of the hot fuel seal sleeve and reduced dynamic response. These problems are solvable with continued development. Good high-temperature fuel sealing was obtained with the take-apart design feature.

5.3.3. Injector Actuation. The experimental fuel injector was designed to be actuated by a hydraulic pulse from a conventional engine-driven diesel fuel injection pump in a closed-loop system separate from the engine fuel supply circuit. Because the OEM fuel injection pump for the test engine did not have provisions for dynamic injection timing control, a special mounting fixture and adapter shaft were built to drive a conventional Bosch VE rotary type fuel injection pump directly off the engine crankshaft. The VE pump was selected for its hydraulically actuated timing advance mechanism and spill metering features. The advance piston is actuated by pump case pressure which is a linear function of engine speed. To provide independent timing control, the case pressure supply passage to the timing piston was plugged, and a special closed hydraulic circuit was built to independently control pressure supplied to the advance piston. This circuit consisted of a pump, reservoir, and a pilot actuated relief valve that was remotely controlled from the test cell console. This control system provided an 18 crank angle degree (CAD) dynamic start of injection timing window during engine operation. By static adjustment of the VE actuation pump, the 18-degree window could be indexed $\pm$20 CAD from TDC. The VE pump governor and spill metering sleeve were adjusted to provide a maximum fuel injection duration of 50 CAD. Both the actuation circuits and the timing control circuit were charged with VISCOR 1487 calibration liquid.

5.3.4. Fuel Pressurization. To provide high-pressure fuel to the fuel heater, an existing ERC high-pressure fuel source unit was recomissioned and modified for this application. This unit consists of a compressed air-driven intensifier, a surge chamber, return float tank, and associated remote controls. Limit switches monitor hydraulic piston frequency over a constant stroke and provide a measurement of fuel flow. The unit has a 7,000 PSI maximum pressure capability.

5.3.5. Fuel Heater and Deposit Removal System. The high-pressure liquid fuel at room temperature supplied by the pressurization unit described in Section 5.3.4. was passed through a given coiled length of 0.25 in. OD by 0.09 in. ID 316 type stainless steel tubing before reaching the injector hot fuel section. A DC current passing through the tubing provided resistive type heating of the tube to sufficient temperature to provide adequate fuel heating. Over the test program the overall tubing length was varied between 8 and 20 feet. Most of the tubing length was in a coil pack in a steel container case near the engine. This case was filled with

nitrogen during engine testing to provide an extra margin of safety in case the hot tube leaked. The transfer tube between the heater case and the injector was 16 in. long and contained the only take-apart connector fitting. This fitting was a Snotrik SS460-6 union. An unusually severe hot fuel deposit problem 1 to 8 in. upstream from this fitting was mitigated by the insertion of three 0.028 in. diameter stainless steel wires to increase flow velocity.

The DC power supply was a Sorensen Model DCR-40-125A with a 0-40 VDC, 0-125 ampere, 5000 watt maximum output from a 220 VAC three-phase input. The positive buss was located at the beginning of the heater coil, and the negative ground buss was on the injector, so the transfer tube was included in the heating circuit.

The entire length of the heater tubing and the injector hot section were insulated with shapeable felt alumina ceramic fiber insulation. The insulation thickness varied between 0.5 to 1.0 in., depending on location.

An oxidation type fuel deposit removal system was incorporated into the fuel heater. Deposits were removed by using the following sequential procedure:

- Purge with 20 PSI $N_2$ to force fuel into cooler circuit if heater was not plugged.
- Purge with 2,000 PSI $N_2$ to initiate flow if the heater was plugged.
- After $N_2$ flow was established, 80 PSI compressed air was applied.
- With air flowing, electrically heat tube to 1,000-1,200°F for 20-30 minutes to oxidize all fuel deposits.
- If the 2,000 PSI $N_2$ could not establish flow, 2,000 PSI air with the 1,000-1,200 F tube temperatures were used to establish flow.

## 5.4 Instrumentation and Data Reduction

5.4.1. Temperature. Type K Chromel-Alumel thermocouples were used to measure all temperatures. Eleven thermocouples were bonded to the hot fuel tube outside wall throughout the heating circuit. The thermocouple located on the hot tube OD just before entering the injector body flange was chosen as the reference temperature to indicate fuel temperature. Later in the program, a thermocouple was located directly in the hot fuel flow stream within 0.5 in. of the reference OD thermocouple. These two temperatures correlated within 5%. Inlet air temperature, oil temperature, and exhaust gas temperature were also measured.

5.4.2. Pressure. A Kistler Type 6121 piezoelectric pressure transducer was used to measure engine cylinder pressure. Fuel pressure was measured in the high-pressure fuel supply reservoir with a strain gage-type pressure sensor. Fuel pressure at the

outlet of the fuel heater was not measured because of the cooling requirements for transducers capable of operating at 1,000-3,000 PSI fuel pressure and up to 1,200°F fuel temperature. Minimizing heat loss in the hot fuel transfer tube was a critical item.

5.4.3. Injector Needle Lift. A Bently-Nevada Series 3000 Type 190 proximity probe was used to measure displacement of the actuation piston/hot needle assembly.

5.4.4. Piston Top Dead Center. A magnetic pickup and locator pin on the flywheel were used to record top dead center of the engine piston.

5.4.5. Air Flow. A Meriam Model 509 MC2-2SF laminar air flow meter was used to measure engine air flow.

5.4.6. Fuel Flow. Fuel flow was measured in the high-pressure intensifier by incorporating limit switches and a reset counter. The time needed to accumulate a certain number of piston pumping strokes gave a measurement of fuel flow. At conventional fuel temperatures, the measurement system had a calibration accuracy of ±1%. At high fuel temperatures, however, nonsteady-state flow resulting from fuel compressibility between the point of measurement and point of injection, unpredictable major increases in unrecoverable injector leak-off, and short operation time, combined to cause errors up to 50% in fuel flow measurement. In future efforts, fuel flow should be determined with an air-fuel ratio analyzer integrated into the data acquisition system.

5.4.7. Exhaust Smoke. A Celesco Model 107 smokemeter was used to measure exhaust smoke opacity.

5.4.8. Data Recording. Engine cylinder pressure, injector needle lift, and TDC location were displayed on an oscilloscope and also recorded on magnetic tape. The reference tube wall and in-flow thermocouples, exhaust gas temperature, and exhaust smoke opacity were recorded on a strip chart recorder. All other data was manually recorded on a data sheet.

5.4.9. Data Reduction. Cylinder pressure, injector needle lift, and TDC location were recorded on an analog magnetic tape. The tape recorder was manually turned on and off at the desired engine operating condition. The data tape was taken to the data reduction room for subsequent digitizing and reduction on a Hewlett-Packard Model 1000 computer. Printed output of the data reduction program consisted of:

- Cylinder pressure and injector needle lift vs. time in crank angle degrees
- Needle lift vs. a 2X time base for an improved visual determination of start of effective injector needle lift

- Cylinder pressure vs. cylinder volume. The data reduction program integrated this curve to determine indicated mean effective pressure (IMEP).

- Log of cylinder pressure vs. log of cylinder volume

- Log of cylinder pressure vs. 2X scale of log of cylinder pressure for improved visual determinatin of start of combustion

- Heat release rate vs. time in crank angle degrees. Heat release rate was defined by the equation

$$\frac{dQ}{d\theta} = \frac{1}{k-1}\left(kP\,\frac{dV}{d\theta} + V\,\frac{dP}{d\theta}\right)$$

where

$\frac{dQ}{d\theta}$ = combustion heat release rate (BTU/CAD)
P = cylinder pressure
V = cylinder volume
$\theta$ = crank angle
$k = c_p/c_v$

5.5. Test Fuels

5.5.1. Kerosene. In consultation with Chevron Research Company, Chevron 450 Pearl Kerosene was selected as the first test fuel because of its clean burning performance as a calibration fuel for cetane tests, low end point, low impurities, and 46.5 cetane number which meets the number 2 diesel fuel specification. Typical properties data for Chevron 450 Pearl Kerosene are in Table 5-1.

5.5.2. JP-7. JP-7 (MIL-T-38219) is specialty high-temperature military jet engine fuel for hypersonic aircraft. This fuel was selected after consultation with the U.S. Army Fuels and Lubricants Laboratory at Southwest Research Institute to help mitigate the high-temperature fuel deposit problem encountered with Pearl Kerosene. Specifications and properties data for JP-7 fuel are in Table 5-2.

5.5.3. Methanol. Methanol ($CH_3OH$) was selected as a low cetane alternate because it does not form high-temperature fuel deposits. The cetane number for methanol can not be readily measured but is approximately five. Typical properties data for methanol are in Table 5-3.

5.5.4. Isooctane. Isooctane, specifically 2,2,4-trimethyl-pentane ($C_8H_{18}$), was selected as a single-constituent fuel representative of gasoline. This fuel was 99.95% pure and contained no tetraethyl lead. Typical properties data for isooctane are in Table 5-4.

TABLE 5-1. Typical Properties for Chevron 450 Pearl Kerosene(5).

| | |
|---|---|
| Gravity, °API | 43.0 |
| Gravity, Specific at 60°F | 0.8107 |
| Pounds Per Gallon at 60°F | 6.750 |
| Flash Point TCC°F | 146.0 |
| Flash Point TOC°F | 154.0 |
| Aniline Point°F | 156.0 |
| Kauri Butanol Value | 32.5 |
| Reid Vapor Pressure, PSI | <0.1 |
| Explosive Limits, lower | 0.9 |
| Volume % in Air upper | 5.4 |
| Composition - Volume % | |
| Benzene | 0.02 |
| Toluene/Ethylbenzene | 0.0 |
| Xylene & $C_8$ + Aromatics | 3.6 |
| Naphthenes | 57.4 |
| Paraffins | 39.0 |
| Color Saybolt | +30.0 |
| Distillation, D-86, °F | |
| Initial Boiling Point | 384.0 |
| 10% Recovered | 396.0 |
| 50% Recovered | 409.0 |
| 70% Recovered | 417.0 |
| 90% Recovered | 442.0 |
| Dry Point | 489.0 |
| End Point | 490.0 |
| Spontaneous Ignition Temperature °F | 500.0 |
| Freezing Point °F | -31.0 |
| Molecular Weight, Average | 166.0 |
| Solubility Parameter | 7.2 |
| Refractive Index 20 C | 1.4450 |
| Thermal Conductivity, 60°F BTU/hr/ft/deg°F | 0.084 |
| Heat of Vaporization, BTU/lb. | 108.0 |
| Heat of Combustion, BTU/lb. | 18680.0 |
| Viscosity at 77°F | 1.87 cs, 1.50 cp |
| Viscosity at 100°F | 1.50 cs, 1.19 cp |
| Viscosity at 130°F | 1.18 cs, 0.92 cp |
| Cetane No. | 46.5 |

TABLE 5-2. Properties of JP-7 Fuel.(6)(7)

| Requirements | Specifications | Results |
|---|---|---|
| Color, Saybolt | Report | +30.0 |
| Aromatic, Vol. % | 5 max. | 3.0 |
| Doctor Test | Sweet | Sweet |
| Sulfur, Total wt. % | 0.1 max. | 0.008 |
| Distillation, Initial BP, °F | 360 min. | 391.0 |
| 10% Rec. °F | 385 min. | 409.0 |
| 20% Rec. °F | 403 min. | 416.0 |
| 50% Rec. °F | Report | 418.0 |
| 90% Rec. °F | 500 max. | 441.0 |
| Final BP, °F | 550 max. | 492.0 |
| Residue, vol. % | 1.5 max. | 1.0 |
| Loss, Vol. % | 1.5 max. | 1.0 |
| Flash Point, °F | 140 min. | 160.0 |
| Gravity, API, 60°F | 44-50 | 45.4 |
| Vapor Pressure, 300°F | 3.0 max. | 2.35 |
| Vapor Pressure, 500°F | 48.0 max. | 41.0 |
| Freezing Point, °F | -46 max. | -52.6 |
| Viscosity @ -30°F, cs | 15.0 max. | 12.19 |
| Net Heat of Combustion, Btu/lb | 18,700 min. | 18,732 |
| Luminometer No. | 75 min. | 78.1 |
| Copper Strip Corrosion, 2 hr. @ 212°F | 1B max. | 1B |
| Thermal Stability, JFTOT, 355° | | |
| Pressure Drop, mm. Hg, 5 hrs. | 25.0 max. | 0 |
| Delta TDR Spun | 12.0 max. | 8.0 |
| Existent Gum, mg/100 ml | 5.0 max. | 0.6 |
| Particulate Matter, mg/liter | 0.3 max. | 0.1 |
| Water Reaction, Interface Rating | 1B max. | 1A |
| Separation Rating | 1 max. | 0.5 |
| Water Separometer Index, Modified | 85 min. | 94.0 |
| Fuel Systems Icing Inhibitor | 0.10-0.15 | |
| Top | | 0.145 |
| Middle | | 0.145 |
| Bottom | | 0.145 |
| Thermal Precipitation Rating | B-2 max. | Pass |
| Hydrogen Content Calculated, wt. % | 14.40 min. | 14.419 |
| 2-6-ditertiary-butyl-4 methylphenol, #/1,000 bbls. | 8.4 max. | 8.4 |
| PWA536, PPM | 200-250 | 225 |

TABLE 5-3. Typical Properties for Methanol(3)

| | |
|---|---|
| Formula | $CH_3OH$ |
| Molecular weight | 32.042 |
| Carbon-to-hydrogen weight ratio | 3.0 |
| Carbon, % by weight | 37.5 |
| Hydrogen, % by weight | 12.5 |
| Oxygen, % by weight | 50.0 |
| Boiling point, °F at 1 atm | 148.1 |
| Freezing point, °F at 1 atm | -144.0 |
| Vapor pressure, PSIA at 100°F | 4.6 |
| Specific gravity, 60°F/60°F | 0.796 |
| Liquid density, lb/gal at 60°F and 1 atm | 6.637 |
| Coefficient of expansion, 1/F at 60°F and 1 atm | 0.00065 |
| Surface tension, dynes/cm at 68°F and 1 atm | 22.61 |
| Viscosity, centipoises at 68°F and 1 atm | 0.596 |
| Specific heat of liquid, Btu/lb-F at 77°F and 1 atm | 0.6 |
| Heat of vaporization, Btu/lb at boiling point and 1 atm | 473.0 |
| Heat of vaporization, Btu/lb at 77°F and 1 atm | 503.3 |
| Heat of combustion, Btu/lb at 77°F | |
| Gaseous fuel-liquid $H_2O$ | 10,279.0 |
| Liquid fuel-liquid $H_2O$ | 9,776.0 |
| Gaseous fuel-gaseous $H_2O$ | 9,099.0 |
| Liquid fuel-gaseous $H_2O$ | 8,593.0 |
| Stoichiometric mixture, lb air/lb | 6.463 |

TABLE 5-4. Typical Properties for Isooctane(8)

| | |
|---|---|
| Formula | $C_8H_{18}$ |
| Molecular weight | 114.224 |
| Carbon-to-hydrogen weight ratio | 5.25 |
| Carbon, % by weight | 84.0 |
| Hydrogen, % by weight | 16.0 |
| Oxygen, % by weight | 0.0 |
| Boiling point, °F at 1 atm | 210.63 |
| Freezing point, °F at 1 atm | -161.28 |
| Vapor pressure, PSIA at 100°F | 1.708 |
| Specific gravity, 60°F/60°F | 0.6963 |
| Liquid density, lb/gal at 60°F and 1 atm | 5.795 |
| Coefficient of expansion, 1/F at 60°F and 1 atm | 0.00065 |
| Surface tension, dynes/cm at 68°F and 1 atm | 18.77 |
| Viscosity, centipoises at 68°F and 1 atm | 0.503 |
| Specific heat of liquid, Btu/lb-F at 77°F and 1 atm | 0.5 |
| Heat of vaporization, Btu/lb at boiling point and 1 atm | 116.69 |
| Heat of vaporization, Btu/lb at 77°F and 1 atm | 132.0 |
| Heat of combustion, Btu/lb at 77°F | |
| Gaseous fuel-liquid $H_2O$ | 20,688.0 |
| Liquid fuel-liquid $H_2O$ | 20,556.0 |
| Gaseous fuel-gaseous $H_2O$ | 19,197.0 |
| Liquid fuel-gaseous $H_2O$ | 19,065.0 |
| Stoichiometric mixture, lb air/lb | 15.13 |

## 5.6. Test Procedure

At the beginning of each experiment, the engine was warmed up at normal fuel temperature. Once the oil temperature and fuel supply pressure were stabilized, the injection timing and duration were set to hold a desired IMEP, start-of-combustion point, peak cylinder pressure, and smoke opacity. The fuel heater was then turned on to between 75 and 100% of power supply capacity, and data was recorded initially at 500°F fuel temperature and thereafter at 100°F increments, or when significant observations occurred, up to the maximum test temperature. Most tests with hydrocardon fuels were terminated in the 1,000-1,200°F fuel temperature range because of total blockage of the fuel heater with fuel deposits.

## 5.7. Engine Test Results with High-Temperature Kerosene

Chevron 450 kerosene was used during all engine test efforts with the Level 1 experimental fuel injector design. No substantive engine performance data was obtained with the Level 1 injector because the start of fuel injection could not be accurately measured. For this reason, the Level 2 injector was designed and built.

With the Level 2 experimental fuel injector design, fuel deposit blockage became the limiting factor with 450 kerosene. Effective engine running time at elevated fuel temperatures was 15 to 20 minutes before fuel deposits causing decreasing fuel pressure and subsequent loss of performance and stability, followed in most cases by total blockage of the fuel system. However, as shown in Table 5-5, some encouraging results were obtained. Ignition delay measured by the logP-logV method was reduced by 57% at 900°F fuel temperature before appearing to increase as fuel deposits set in, culminating in complete blockage at 1,150°F fuel temperature. Ignition delay vs. fuel tube temperature up to 900°F is shown in Figure 5-8.

From 85°F to 900°F fuel temperature, the rate of cylinder pressure rise decreased 33% from 51.4 to 34.4 PSI/CAD. Exhaust smoke opacity decreased 65% at 900°F fuel temperature. The smoke opacity continued to decrease in the 1,000-1,100°F fuel temperature range when combustion was retarding because of rapidly decreasing effective injection pressure caused by fuel deposit formation. This test produced the most reliable fuel flow data because the flow was relatively steady and the unrecoverable leak-off was unusually low. The indicated specific fuel consumption (ISFC) data indicates the potential for no thermal efficiency penalty, so the goal of thermal efficiency improvements at reduced maximum cylinder pressure with total engine system development is encouraging.

## 5.8. Engine Test Results with High-Temperature JP-7

All high-temperature JP-7 fuel engine tests were conducted with the Level 2 experimental fuel injector design. With JP-7, the effective engine running time was increased up to 35 minutes before high-temperature fuel deposits plugged the fuel system. The maximum reference fuel pipe temperature reached during the JP-7 testing program was 1,200°F; however, significant data collection was limited to 1,100°F.

TABLE 5-5. Engine Test Results with High-Temperature Kerosene. 2,000 Engine RPM, 2,200 PSI Fuel Supply Pressure, Level 2 Experimental Fuel Injector.

| Fuel Temp. °F | Start of Fuel Injection CAD | IMEP PSI | Ignition Delay ms | Smoke Opacity % | Peak Cyl. Pressure PSIA | ISFC lbm/ihp-hr |
|---|---|---|---|---|---|---|
| 85 | -15.0 | 110 | 0.98 | 7.5 | 1010 | .32 |
| 500 | -15.0 | 108 | 0.79 | 5.5 | 990 | .34 |
| 600 | -14.0 | 105 | 0.67 | 5.0 | 990 | .34 |
| 700 | -14.0 | 91 | 0.62 | 4.2 | 980 | .46 |
| 800 | -13.0 | 102 | 0.45 | 3.7 | 975 | .39 |
| 900 | -13.0 | 100 | 0.42 | 2.6 | 980 | .36 |
| 1,000 | -15.0 | 90 | 1.17 | 0.7 | 940 | .34 |
| 1,050 | -17.0 | 77 | 2.45 | 0.5 | 660 | --- |
| 1,100 | -17.5 | 52 | 3.07 | 0.4 | 660 | --- |
| 1,150 | Total Deposit Blockage - Shutdown | | | | | |

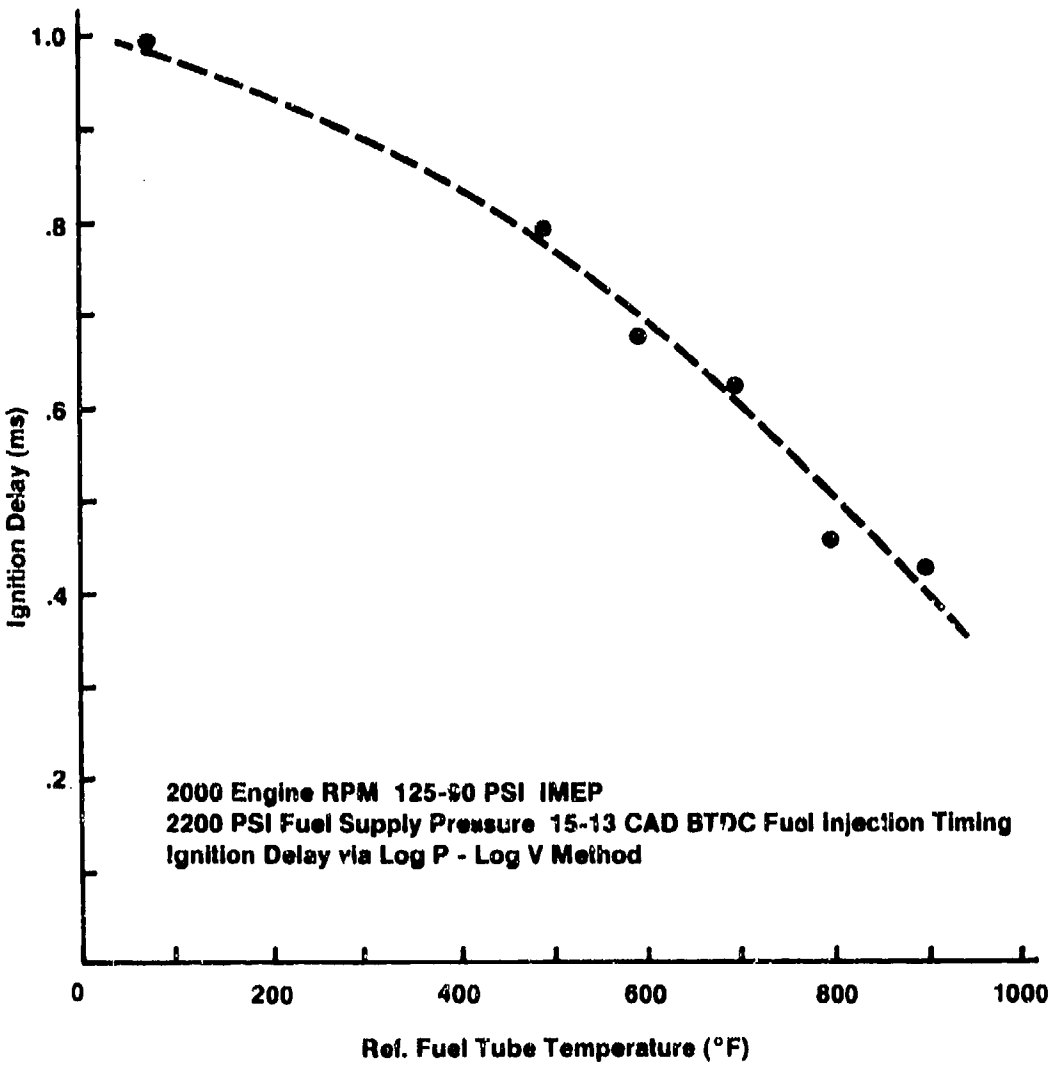


**Figure 5-8. Ignition Delay vs. Fuel Temperature with Chevron 450 Kerosene Fuel**

According to the hypergolic combustion theory, ignition delay should decrease rapidly above a threshold temperature. Such a rapid decrease is shown in Figure 5-9, where ignition delay is seen to decrease 82% from 0.93 ms at 85°F to 0.17 ms at 1,100°F reference fuel tube temperature. The start of combustion was determined by the logP-logV method, and the nonheated baseline data was taken with the experimental fuel injection system. The engine speed was held at 2,000 RPM over a load range of 80-120 PSI IMEP with a fuel supply pressure range of 2,000-2,600 PSI.

When the start of combustion was determined from the heat release curves for the same data points, the ignition delay vs. fuel temperature curve, as shown in Figure 5-10, had the same characteristic and also showed an 82% overall reduction in ignition delay. However, the absolute values were approximately 25% lower. Determination of the start of combustion by the heat release method was more difficult due to curve fluctuations before combustion. The logP-logV method is more accurate.

During the JP-7 fuel test program, the conventional fuel injection system that is original equipment manufacture (OEM) on the Deutz test engine was used to obtain comparison to current state-of-the-art practice. Listed in Table 5-6 is a same-speed-and-load comparison between the OEM fuel system with JP-7 fuel at conventional temperatures and the Level 2 experimental fuel injection system with JP-7 fuel at 1,080°F. This is a comparison between a refined fuel system for this particular engine and a far from optimum experimental fuel system designed to permit high-temperature fuel operation. Nonetheless, for the same 2,000 RPM engine speed and 114 PSI IMEP, the following improvements occurred:

- Ignition delay was reduced by 77%.
- Peak cylinder pressure was reduced by 24%.
- Maximum rate of pressure rise reduced by 91%.
- Exhaust smoke reduced by 67%.

For the two test conditions detailed in Table 5-6, the following figures are presented to further illustrate the effect of high-temperature fuel: Figure 5-11, Cylinder Pressure vs. Time; Figure 5-12, Cylinder Pressure vs. Volume; Figure 5-13, Log Pressure vs. Log Volume; and Figure 5-14, Heat Release Curves. These curves graphically illustrate the reduction in peak cylinder pressure, reduction in rate of cylinder pressure rise, elimination of the usual initial heat release spike, and the increased combustion duration. Combustion duration is longer with hot fuel because injection duration is longer. On the other hand, combustion is actually faster since combustion duration minus injection duration is 25% shorter with hot fuel, as shown in Figure 5-14.

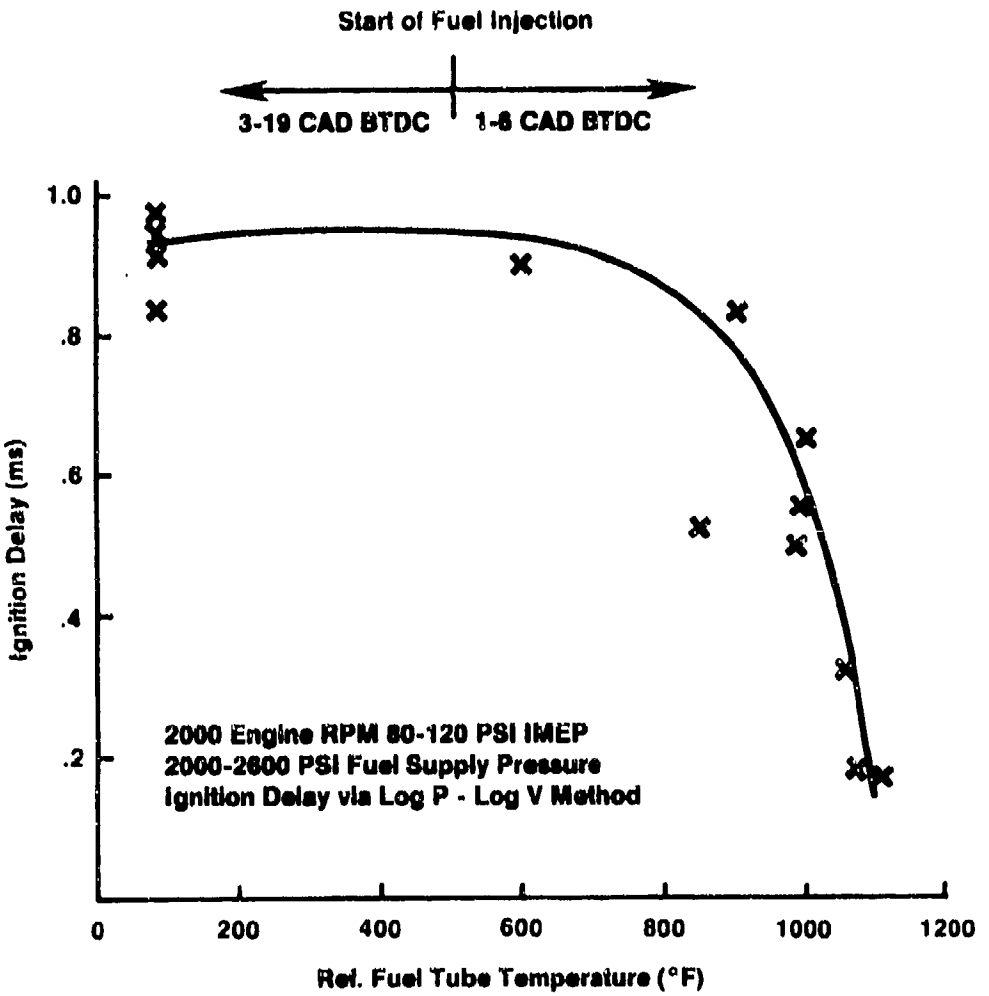


**Figure 5-9. Ignition Delay by Log P - Log V Method vs. Fuel Temperature with JP-7 Fuel**

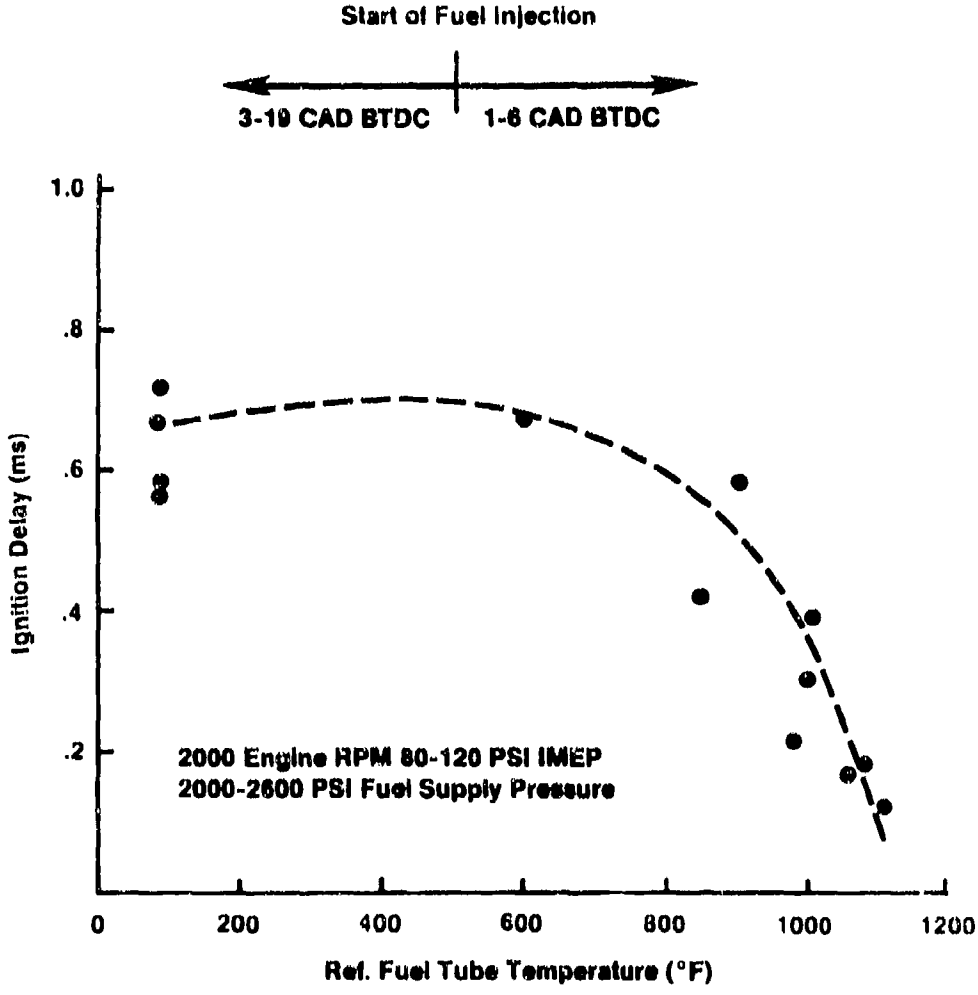


**Figure 5-10. Ignition Delay by Heat Release Method vs. Fuel Temperature with JP-7 Fuel**

TABLE 5-6. Engine Performance Comparison Between High-Temperature Fuel Test and OEM Fuel System Baseline Test with JP-7 Fuel

| | OEM Fuel Injection System | Level 2 Experimental High-Temperature Fuel Injection System |
|---|---|---|
| Engine Speed (RPM) | 2,000 | 2,000 |
| IMEP (PSI) | 114 | 114 |
| Fuel Pressure (PSI) | 4,000 maximum | 2,130 steady supply |
| Ref. Fuel Temperature ($^{o}$F) | 85 | 1,080 |
| Start of Fuel Injection (CAD) | -11.0 | -2.3 |
| Injection Duration (CAD) | 17.2 | 42.3 |
| Start of Combustion (CAD) | -1.3 | 0.0 |
| Combustion Duration (CAD) | 37.2 | 57.3 |
| Ignition Delay (CAD/ms) | 9.7/0.81 | 2.3/0.19 |
| Peak Cylinder Pressure (PSI) | 940 | 710 |
| Maximum Rate of Pressure Rise (PSI/CAD) | 43 | 4 |
| ISFC (lbm/ihp-hr) | .361 | --- |
| Exhaust Smoke (% opacity) | 3.0 | 1.0 |

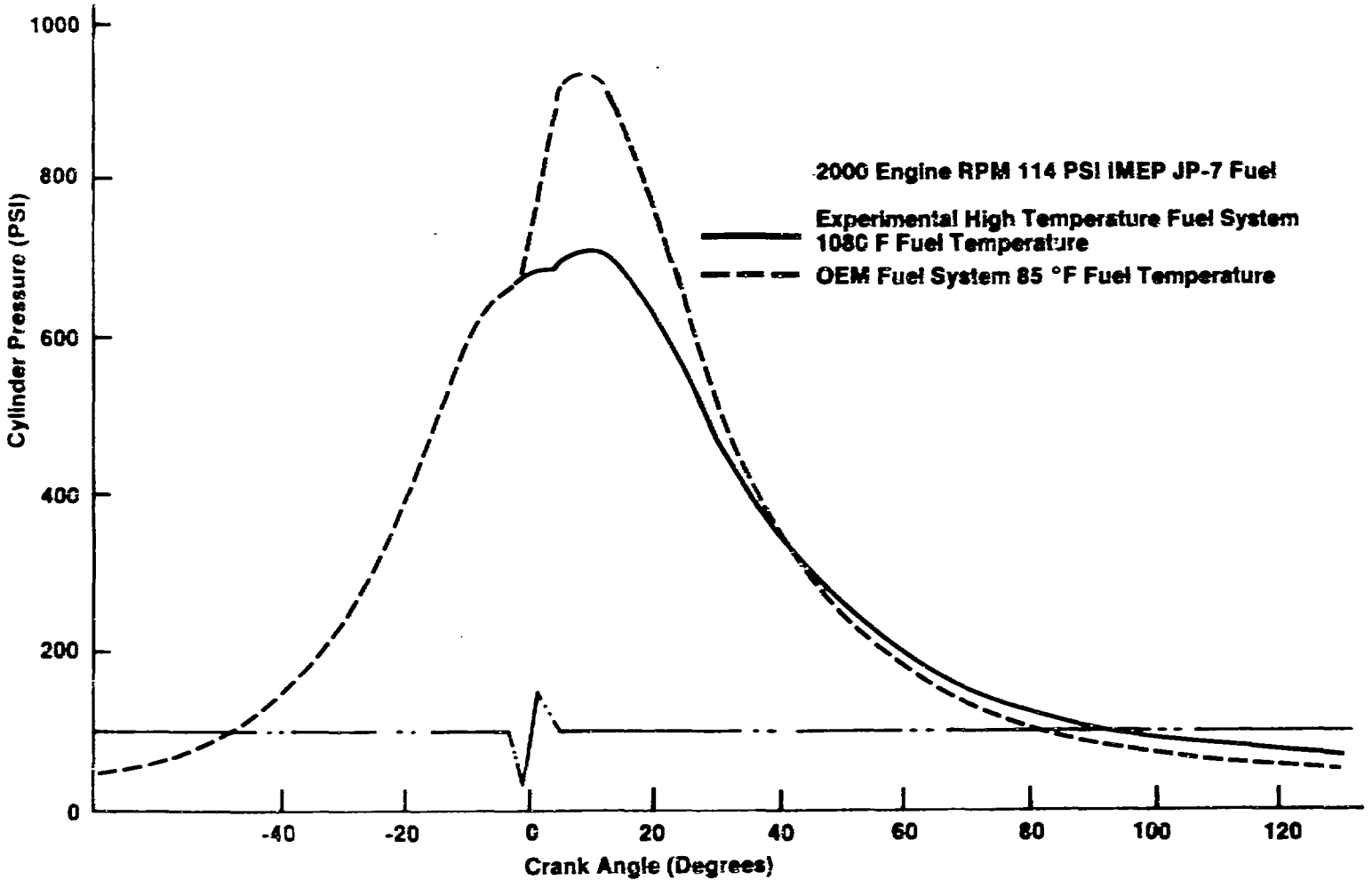


Figure 5-11. Cylinder Pressure vs. Time Comparison of High Temperature Fuel Data vs OEM Baseline

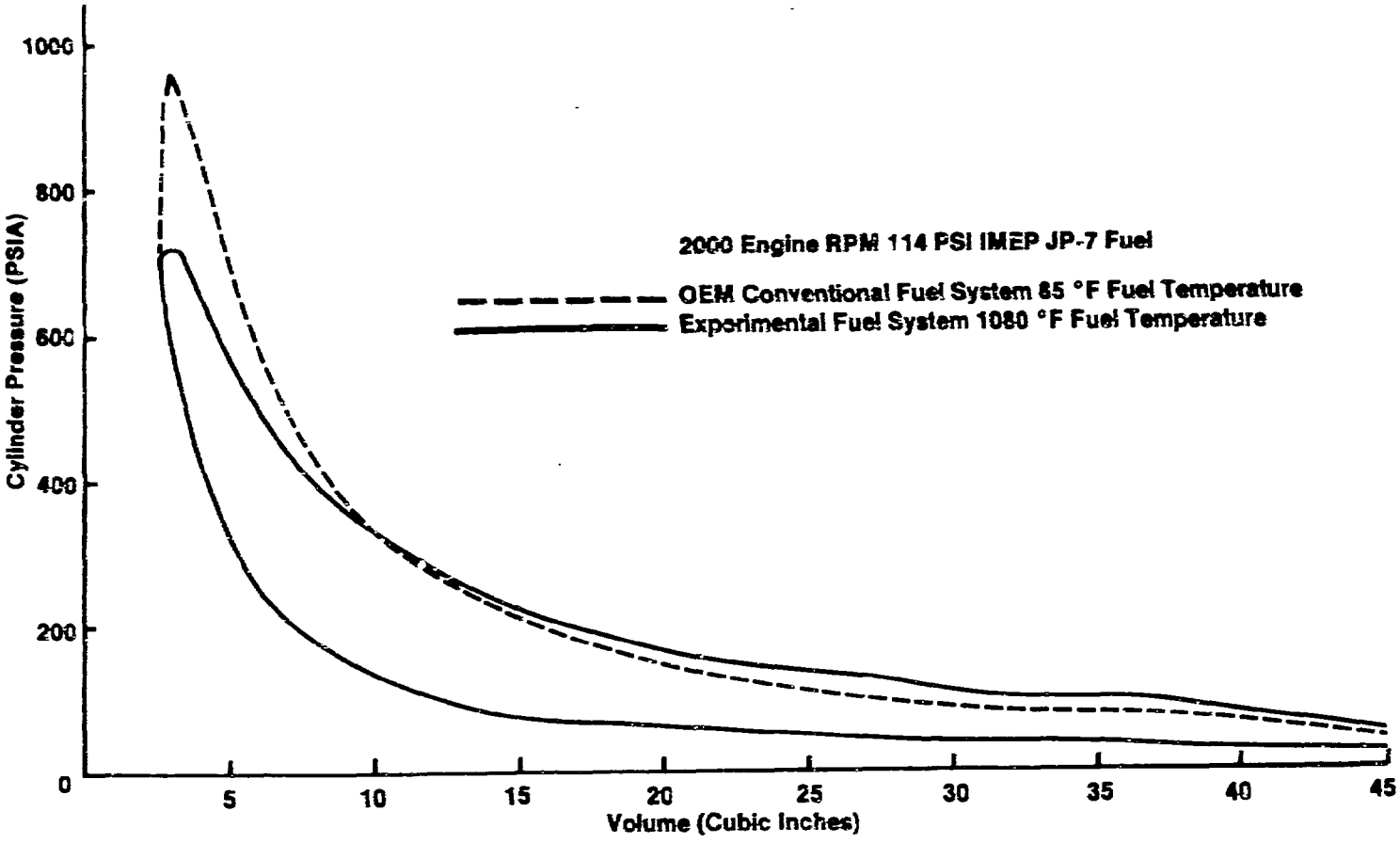


**Figure 5-12. Cylinder Pressure vs. Volume Comparision of High Temperature Fuel Data vs. OEM Baseline**

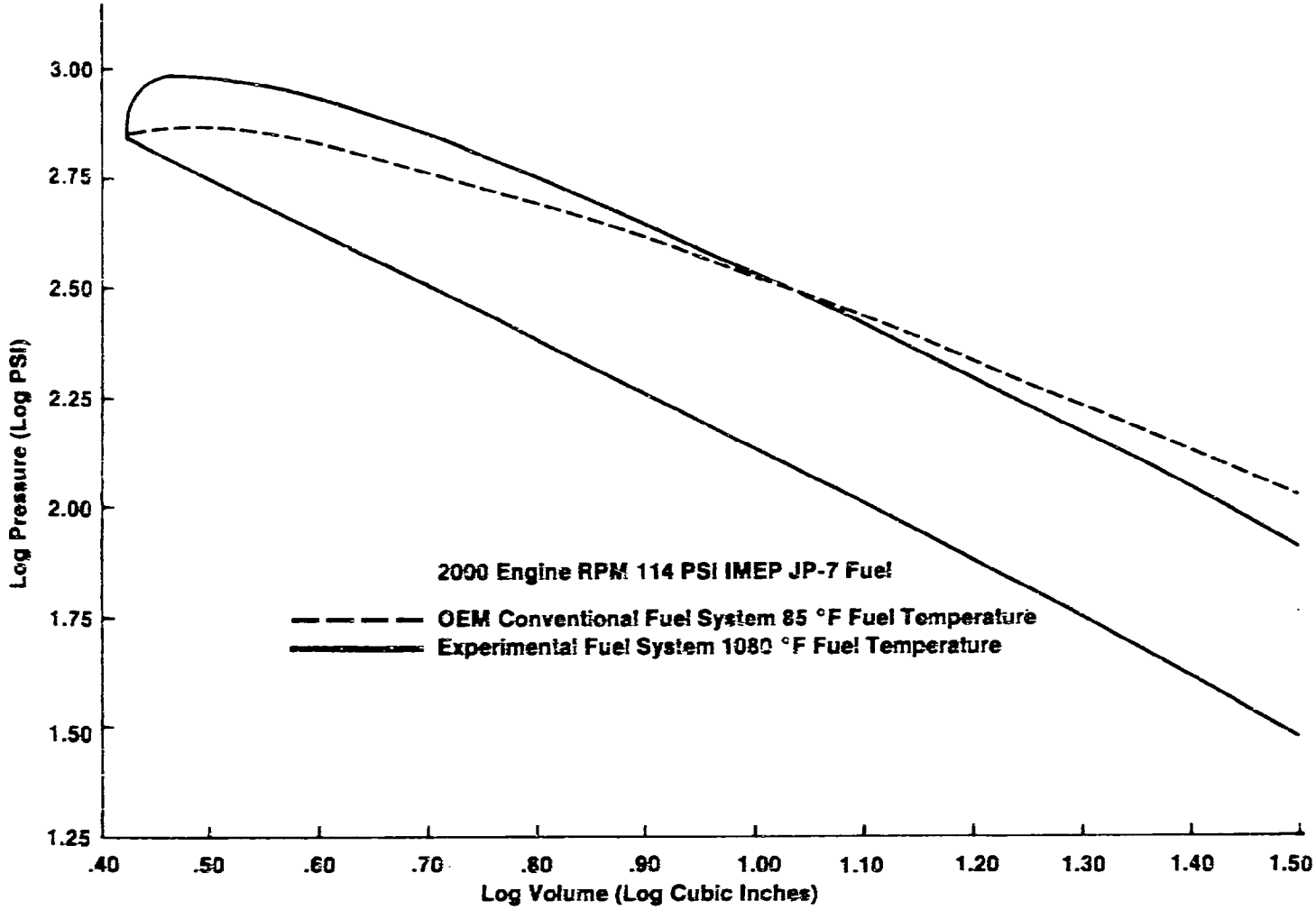


Figure 5-13. Log P vs. Log V Comparison of High Temperature Fuel Data vs. OEM Baseline

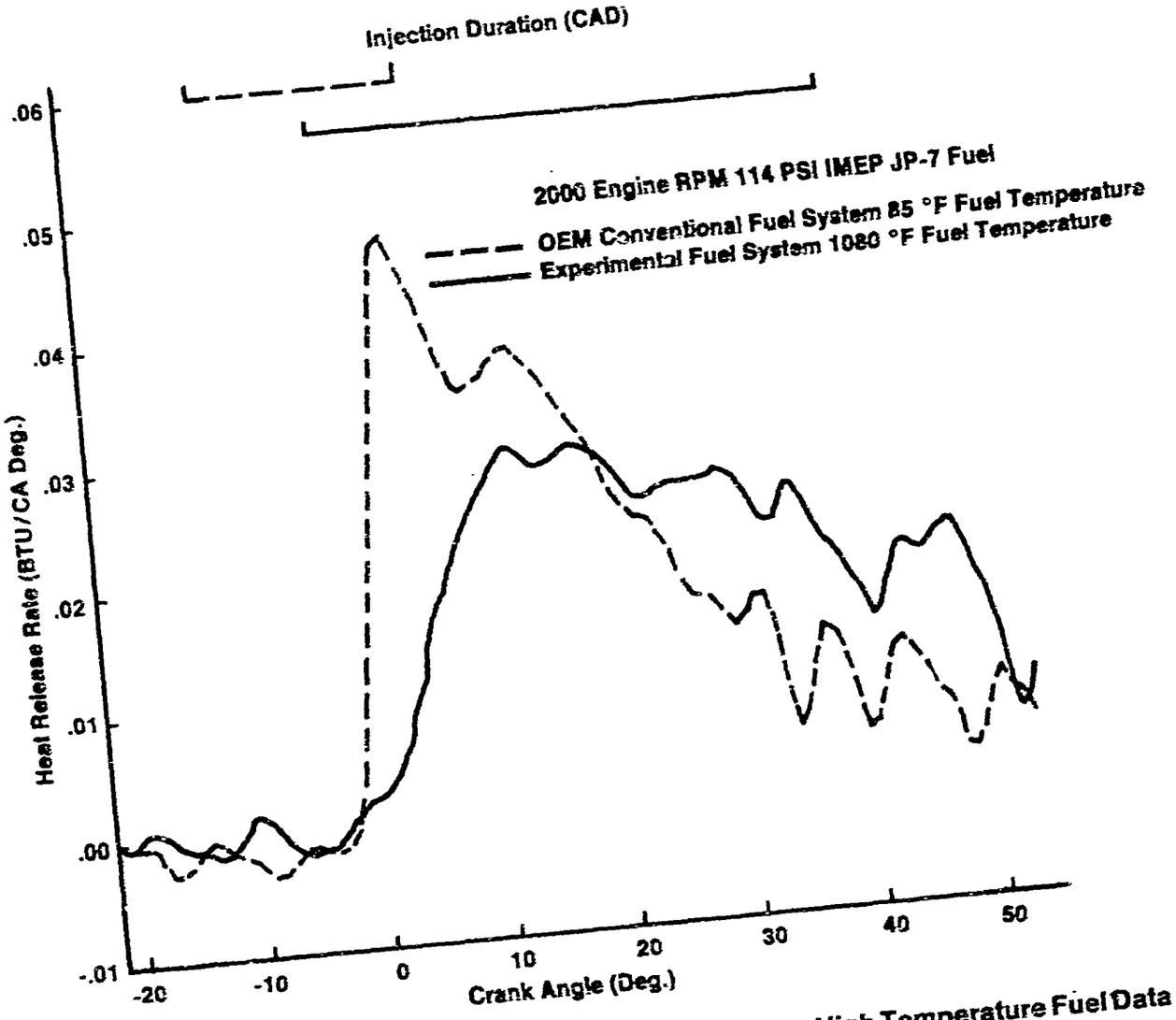


Figure 5-14. Heat Release Rate vs. Time Comparison High Temperature Fuel Data and OEM Baseline

A test was conducted using JP-7 fuel with the objective of holding the peak cylinder pressure at 700 ±20 PSI as the fuel was heated from room temperature to the high-temperature limit. The OEM fuel system could not maintain a load greater than 20 PSI IMEP without exceeding 700 peak cylinder pressure. Only by means of late and relatively long fuel injection duration with the experimental fuel system, could the 700 PSI peak cylinder pressure limit at 85 PSI IMEP load be kept with room temperature fuel, resulting in a high smoke opacity of 14%.

A plot of smoke opacity and IMEP vs. referenced fuel tube temperature for this test in Figure 5-15. The smoke opacity decreased rapidly above 600°F fuel temperature and approached zero in the 1,000-1,100°F reference fuel temperature range. Smoke is so low even with the long and late fuel injection duration, which is indicative of improved combustion quality. This is reflected in the dramatic 35% IMEP increase at near zero smoke opacity. The IMEP increase between the same fuel injection timing and duration for the last two data points results from increased fuel mass flow caused by the temporary break-up of flow-restricting fuel deposits. Reliable fuel flow data was not obtained during this test. The fuel heater plugged with fuel deposits soon after collection of the last data point.

It was originally intended to reduce the nominal compression ratio to a level that would not produce compression ignition at normal fuel temperatures, and then demonstrate that ignition and combustion would occur if the fuel was sufficiently preheated. In order to prevent an accumulation of unburned fuel in the exhaust system, the procedure envisaged was to motor the engine while preheating the fuel at zero fuel flow rate. Once the fuel temperature reached about 800°F, injection would be initiated. Preliminary tests showed, however, that fuel deposits were severe at zero fuel flow and would not give meaningful test data. Consequently, this experiment was not carried out.

## 5.9. Engine Test Results with High-Temperature Methanol

5.9.1. Methanol. For initial checkout testing with neat methanol fuel, no changes were made to the Level 2 injector design. All methanol tests were conducted at 2,000 engine RPM and 2,000-3,000 PSI fuel supply pressure. There was no combustion with room temperature methanol. Even in the 800-1,200°F fuel tube temperature range, no combustion was detected. Subsequent calculations indicated that the existing total nozzle orifice area was too small for significant energy input of supercritical methanol, and that a near tenfold increase in orifice area was needed. With the welded lower injector assembly, the maximum orifice increase was obtained by grinding off the nozzle sac tip, providing an area increase factor of 5.1 at the expense of a single downward directed orifice. With the enlarged single orifice, the engine would again not operate with room temperature fuel. At 2,000-2,200 PSI fuel supply pressure and 15-18 CAD BTDC fuel injection timing, the 400-600°F fuel temperature produced erratic engine operation with the ignition delay varying in the 1.0 to 1.8 ms range. In the 800-1,200°F fuel temperature range, no combustion was observed. In the 900-1,330°F fuel temperature range, the engine again ran erratically. These ignition delay ranges are shown in

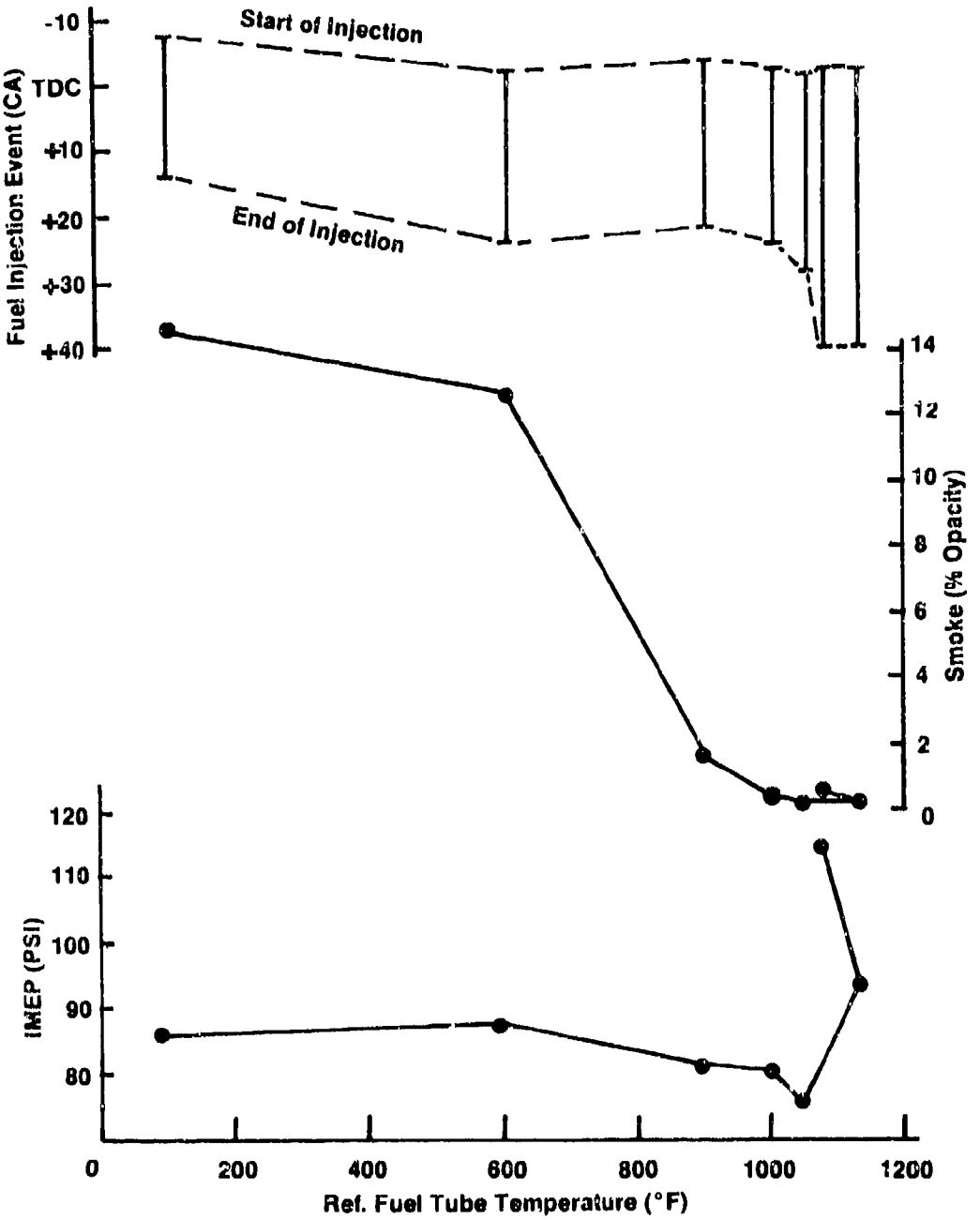


2000 Engine RPM 2150 PSI Fuel Supply Pressure
700 ± 20 PSI Peak Cylinder Pressure JP-7 Fuel

**Figure 5-15. IMEP and Smoke vs. Fuel Temperature at Constant Peak Cylinder Pressure**

Figure 5-16. No detrimental high-temperature fuel deposits were encountered with methanol.

During some methanol tests, no combustion was detected up to 1,300°F reference fuel temperature. The results of this test effort prove that the chemical kinetics of methanol should be investigated.

## 5.10. Engine Test Results with High-Temperature Isooctane

The Level 2 experimental fuel injector was restored to the original four 0.0105 in. diameter orifices. All isooctane tests were run at 2,000 engine RPM and 2,000-2,500 PSI fuel supply pressure. As expected, the engine would not operate on isooctane at normal temperature. Erratic combustion started during the initial heated isooctane test as the reference fuel temperature reached 1,000°F. Unfortunately, the temperature then declined rapidly due to increased fuel leakage which exceeded the heater's capacity to maintain temperature. It was later determined that the leakage was caused by severe galling of the hot needle seal sleeve, so a new 17-7PH stainless steel seal sleeve was installed. The next test was ended at 800°F reference fuel temperature due to fuel deposit blockage in the heater.

In an attempt to increase the operating time at elevated temperatures, a series of tests were run to evaluate reduced fuel residence time. With the injector installed in a nitrogen filled collector/cooler fixture outside the engine, the effective heater pipe length was varied by changing the location of the positive heater cable buss clamp. Acceptable fuel temperatures could be reached with the effective heater coil length reduced from 20 feet to 9.2 feet. During the next test at 1,030°F fuel reference temperature, definitive combustion was observed for 2 to 3 seconds just before a rapid loss of fuel rail pressure which caused shutdown of the engine. Unfortunately, the analog tape recorder could not be started quickly enough to record this. It was later determined that the pressure loss was caused by failure of the ceramic cement that secured the hot needle seal sleeve and by erosion of the seal sleeve bore surface. A new 316 stainless seal sleeve was installed.

The next test was terminated at 700°F reference fuel temperature due to deposit blockage in the fuel heater. This blockage occurred in a 120 degree section of one coil in the hottest section of the heater coil. These deposits could not be removed by the established pressure/oxidation method. Sectioning and inspection of the plugged heater tube revealed several occurences where hard agglomerated carbon particles bonded firmly to the wall surface and extended across the inside cross-sectional area. In Figure 5-17, a photograph of the sectioned heater tube shows the firm deposit blockage along with a sample of loose deposit material that was scrapped out of the heater tube.

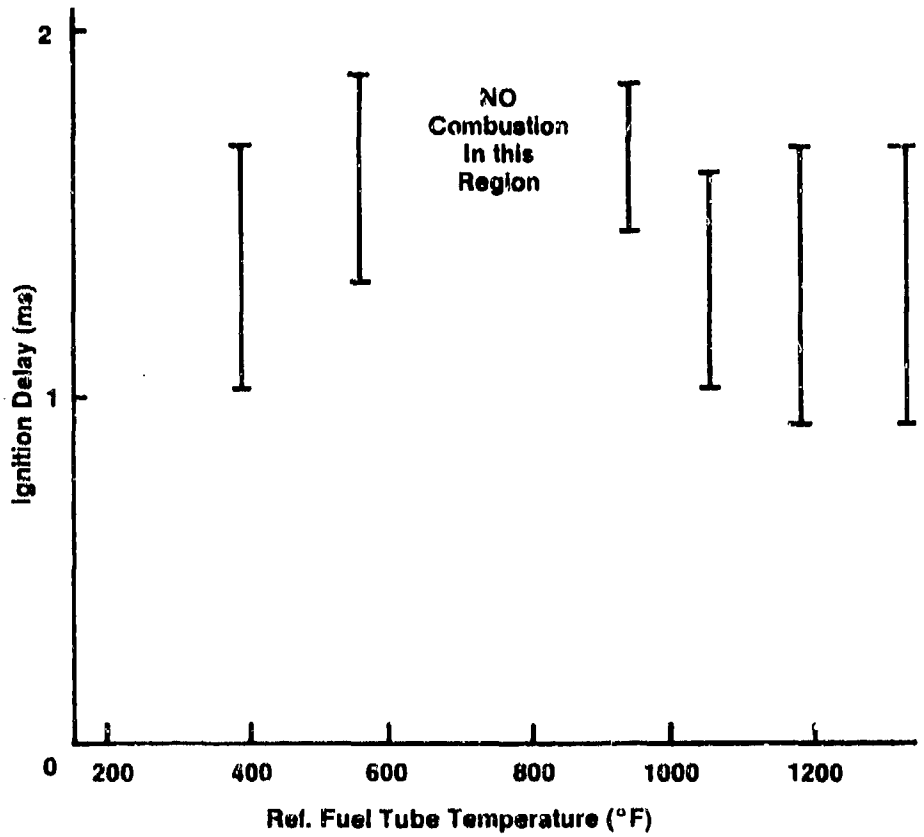


**Figure 5-16. Ignition Delay vs. Fuel Temperature with Neat Methanol**

**Figure 5-17. Sectional View of Heater Tube Plugged with High Temperature Fuel Deposits**

A new 316 stainless steel heater coil with a maximum effective length of 8.4 feet was fabricated, and the new take-apart Level 3 experimental fuel injector was installed. Four heated isooctane tests were terminated in the 500-800°F fuel temperature range due to severe galling and sticking of the hot needle and seal sleeve. Erratic combustion was observed in the 750-800°F fuel temperature range but was insufficient to be documented. 316 and 17-7PH stainless steel sleeves, high-temperature lubricants, and 2% SAE 30 weight oil in the fuel were tried to mitigate the seal sleeve galling problem which usually occurred before high-temperature fuel deposits became the limiting factor.

## LIST OF REFERENCES

(1) Hoppie, L. O. "Pyrophoric Combustion in Internal Combustion Engines," Eaton Technical Report No. 7845, 1978.

(2) Hoppie, L. O. "The Influence of Initial Fuel Temperature on the Ignition Delay of Fuel Injected into Air," Eaton Technical Report No. 7846, 1978.

(3) Hoppie, L. O. "The Influence of Fuel Temperature on Ignition Delay," SAE Paper No. 820356, 1982.

(4) Maxwell, J. B. "Data Book on Hydrocarbons," Krieger Publishing Co., New York, Ninth Printing, p.123, 1968.

(5) "Chevron 450 Pearl Kerosene Bulletin," Chevron Research Co., Richmond, California, 1981.

(6) "Certificate of Analysis" for JP-7 MIL-T-38219 Fuel, Batch 2-83-CBG, Tank No. 78, Ashland Oil Co., Catlettsburg, Kentucky, 1983.

(7) "Aviation Fuels Handbook," Coordinating Research Council, CRC Report No. 530, 1983.

(8) Ebersole, G. D. and Manning, F. S. "Engine Performance and Exhaust Emissions: Methanol vs. Isooctane," SAE Paper No. 720692, 1972.

## BIBLIOGRAPHY


Austen, A., and Lyn, W., "Relation Between Fuel Injection and Heat Release in a Direct-Injection Engine and the Nature of the Combustion Processes," I. Mech. E, No. 1, 1960-1961, p. 47.

Borman, G. L. and Krieger, R. B., "The Computation of Aparent Heat Release for Internal Combustion Engines," ASME Paper No. 66-WA/DGP.

Ekchian, A.; Heywood, J. B. Kort, R. T.; and Mansouri, S. H., "Divided-Chamber Diesel Engine, Part II: Experimental Validation of a Predictive Cycle - Simulation and Heat Release Analysis," SAE Paper No. 820274, 1982.

"Final Report for Study of Turbojet Main Burners for use with Contaminated Fuel," Pratt & Whitney Aircraft, Bureau of Naval Weapons, Contract NOW 63-0489-d, 1963.

Flytzani-Stephanopoulos, M. and Voecks, G. E., "Autothermal Reforming of Aliphatic and Aromatic Hydrocarbon Liquids," JPL, International Association for Hydrogen Energy, Vol. 8, No. 7, 1983.

Gerrish, H. C. and Ayer, B. E., "Influence of Fuel-Oil Temperature on the Combustion in a Prechamber Compression Ignition Engine," NACA TN 565, 1936.

Goudie, G. O.; Prentice, B. W.; Stotter, A.; and Whitehouse, N. D., "Method of Predicting Some Aspects of Performance of a Diesel Engine Using a Digital Computer," I. Mech. E., Vol. 176, No. 9, 1962, p. 195.

Grigg, H. C. and Syed, M. H., "The Problem of Predicting Rate of Heat Release in Diesel Engines," I. Mech. E. Proceedings 1969-1970, Vol. 184, Part 3J, Diesel Engine Combustion, p. 192.

Hawksley, G. J. and Anderton, D., "Studies Into Combustion and Noise in Turbocharged Engines," I. Mech. E. Conference Publication, Turbocharging and Turbochargers, 1978, p. 183.

Heywood, J. B.; Mansouri, S. H.; and Radhakrishnan, K., "Divided-Chamber Diesel Engine, Part I: A Cycle-Simulation Which Predicts Performance and Emissions," SAE Paper 820273, 1982.

Hoppie, L. O., "The Influence of Initial Fuel Temperaure on Ignition Delay," Eaton Corporation, Engineering & Research Center, SAE Paper No. 820356, 1982.

Jain, B. C.; Rife, J. M.; and Keck, J. C., "A Performance Model for the Texaco Controlled Combustion, Stratified Charge Engine," SAE Paper No. 760116, 1976.

Lancaster, David R.; Krieger, Roger B.; and Lienesch, John H., "Measurement and Analysis of Engine Pressure Data," SAE Paper No. 750026, 1975.

Lyn, W. T., "Calculations of the Effect of Rate of Heat Release on the Shape of Cylinder-Pressure Diagram and Cycle Efficiency," I. Mech. E., No. 1, 1960-1961, p. 34.

Lyn, W. T., "Study of Burning Rate and Nature of Combustion in Diesel Engines," Ninth Symposium (International) on Combustion, The Combustion Institute, 1962, p. 1069.

McFarland, R. A. and Wood, C. D., "An Analog Heat Release Computer for Engine Combustion Evaluation," SAE Paper 760553, 1976.

Roback, R., et al, "Deposit Formation in Hydrocarbon Fuels," United Technologies Research Center, Journal of Engineering for Power, Vol. 105, January 1983.

Singh, Trilochan and Sourakomol, Kosol, "Mathematical Modeling of Combustion Process in a Spark Ignition Engine," SAE Paper No. 790354, 1979.

Spadaccini, L. J., "Autoignition Characteristics of Hydrocarbon Fuels at Elevated Temperatures and Pressures," ASME Paper No. 76-GT-3, 1976.

Szetela, E. J., "Deposits from Heated Gas Turbine Fuels," United Technologies Research Center, ASME Paper No. 76-GT-9, March 1976.

Szetala, E. J. and Chiappetta, L., "External Fuel Vaporization Study - Phase I Report," United Technologies Research Center for NASA Lewis Research Center, NASA CR159850, June 1980.

Szetela, E. J. and TeVelde, J. A., "External Fuel Vaporization Study - Phase II Final Report," United Technologies Research Center for NASA Lewis Research Center, NASA Contractor Report 165513, November 1981.

TeVelde, J., et al, "Alternate Fuel Deposit Formation," United Technologies Research Center, AGARD Propulsion and Energetics Panel 62nd Symposium, October 1983.

Whitehouse, N. D. and Way, R., "Rate of Heat Release in Diesel Engines and its Correlation with Fuel Injection Data," I. Mech. E. Proceedings 1969-1970, Vol. 184, Part 3J, Diesel Engine Combustion, p. 17.

# APPENDIX A

SAE Paper No. 820356 by
Dr. L. O. Hoppie of Eaton Corporation

Reprinted with Permission of SAE

The Engineering Resource For Advancing Mobility

400 COMMONWEALTH DRIVE WARRENDALE, PA 15096

# SAE Technical Paper Series

820356

# The Influence of Initial Fuel Temperature on Ignition Delay

L. O. Hoppie
Corporate Research Dept.
Eaton Engrg. & Research Center
Southfield, MI

Reprinted from P-107—
"Diesel Engine Combustion, Emissions, and Particulates"

International Congress & Exposition
Detroit, Michigan
February 22-26, 1982

820356

# The Influence of Initial Fuel Temperature on Ignition Delay

L. O. Hoppie
Corporate Research Dept.
Eaton Engrg. & Research Center
Southfield, MI

ABSTRACT

A new model of ignition delay is formulated and the equations which govern ignition are presented. The model is based on fuel molecules having discrete allowed energy levels, and interprets radicals simply as additional allowed energy levels. Using such a model, the initial fuel temperature can readily be accounted for and its effect on ignition delay predicted. Equations for the general multi-level system are presented, as is the detailed solution for the simple two-level system. Theoretical results predict that the ignition delay can be made arbitrarily small and essentially independent of air temperature if the fuel is sufficiently preheated.

NUMEROUS INVESTIGATIONS have been performed on the ignition delay of fuel injected into air. The majority of these works concentrated on the effects of the initial air temperature and pressure on the ignition delay, since initial fuel temperatures as high as 500°K had little or no effect on ignition delay. Some investigators, however, preheated fuel considerably above 500°K and found significant decreases in ignition delay.

For example, Gerrish and Ayer (1)* used a compression ignition engine of swirl chamber design to measure, among other things, the ignition delay of fuel preheated to temperatures as high as 672°K (750°F). At this condition, an ignition delay of approximately six crank angle degrees was observed, as compared with approximately ten crank angle degrees of delay when the fuel temperature was 324°K (124°F).

In a study of the effects of fuel vaporization on combustion in a turbojet combustion chamber, Holmes et al. (2) made visual observations on the flame which resulted when fuel, preheated prior to leaving the nozzle, was burned in the open atmosphere with no direct air movement. They observed that a small distance existed between the end of the nozzle and the visible flame when room temperature fuel was used, and that this distance decreased as the initial temperature of the fuel was increased. No space could be observed between the nozzle and the visible flame for fuel temperatures above 617°K (650°F).

More recently, Spadaccini (3) reported some profound results obtained in a steady-flow test facility in which the ignition delay of various fuels was measured as a function not only of air temperature and pressure, but also as a function of initial fuel temperature to temperatures as high as 700°K (800°F). Spadaccini's Figure 11 is presented here as Figure 1, where a significant effect of initial fuel temperature can be seen. The full implications of his results, however, can best be observed by plotting the ignition delay versus reciprocal air temperature, as has been done in Figure 2. Notice that the curvature of the data labeled $T_F$ = 800°F is different from the curvature of the other data. DeZubay's modified two-stage mechanism (4), proposed as an explanation of Spadaccini's results, fails to explain the high fuel temperature data since such a mechanism cannot predict the observed reversal in curvature.

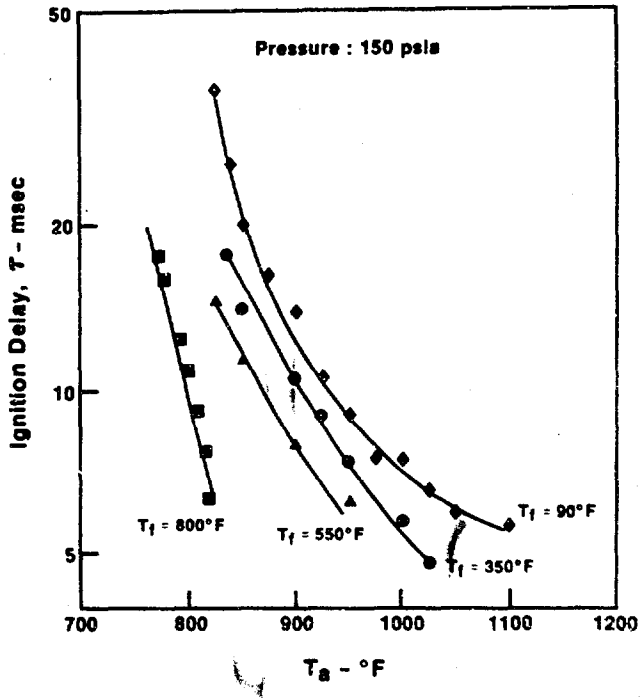


Fig. 1 - Ignition Delay Versus Air Temperature for Various Initial Fuel Temperatures (3)

*Numbers in parentheses designate References at end of paper.

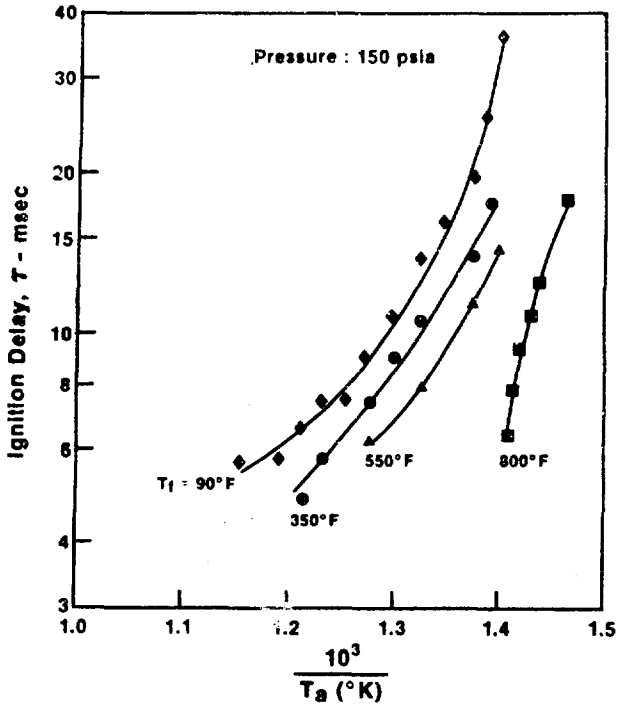


Fig. 2 - Ignition Delay Versus Reciprocal Air Temperature for Various Initial Fuel Temperatures (3)

In this paper, a new model of ignition delay which includes the effect of initial fuel temperature is presented. As will be shown, the model predicts many of the observed trends in ignition delay, including the reversal in curvature observed by Spadaccini, as the fuel is sufficiently preheated.

## THE IGNITION DELAY MODEL

It is well known that a fuel molecule (or any molecule, for that matter) has discrete energy levels (5) corresponding to various longitudinal, rotational and torsional modes of oscillation. For an assembly of $N_o$ such fuel molecules in thermal equilibrium at normal temperatures, the number of molecules in each energy level would be governed by Boltzmann statistics. It is also known that in a combusting mixture, radicals of the original fuel molecule can be observed in front of the flame front, and furthermore, that their density increases drastically as the flame front approaches, i.e., as the temperature increases (6). It is usually assumed that these radicals exist only when combustion is apparent or imminent. However, if the fuel radicals are interpreted simply as additional allowed energy states of the fuel molecule, it follows that in thermal equilibrium there will be a finite number of molecules in these states even if combustion is neither apparent nor imminent.

Let the radical states be referred to as excited states of the fuel, and call the other states the ground states. The following hypotheses are now made:

1. molecules in the ground states cannot react with oxygen.

2. molecules in the excited states will react with oxygen at rates dependent on the concentration of oxygen and the concentration of molecules in the various excited states.

Note that this is rather like the well-known picture of a semiconductor in which the energy levels corresponding to the lowest excited state and the highest ground state are the conduction and valence bands, respectively. Analogies between fuel and a semiconductor can also be made regarding the two hypotheses stated above, and have to do with the electrical current carried by a semiconductor:

1. electrons in the valence band produce no current.

2. electrons in the conduction band produce a current which is dependent on the number of conduction band electrons and the applied voltage.

The analogies between a semiconductor and a fuel molecule which can be drawn as a result of the model are summarized in Table 1 below.

Table 1 - Analogies Between a Semiconductor and a Fuel Molecule

| Semiconductor | Fuel |
|---|---|
| Electrons can Exist at any Temperature in the Valence and Conduction Bands. | Fuel Molecules can Exist at any Temperature either as "Normal" Molecules or as Radicals. |
| The Conduction and Valence Bands are Separated by an Energy Gap, $E_g$. | The Lowest Radical State and the Highest "Normal" State are Separated by an Amount Called the Activation Energy. |
| Only Electrons in the Conduction Band can React with an Electric Field to Cause Current to Flow. | Only Fuel Radicals can React with Oxygen to Cause Heat to be Released. |

Using this model, the simplest case would be when only one excited state and one ground state exist, as shown in Figure 3.

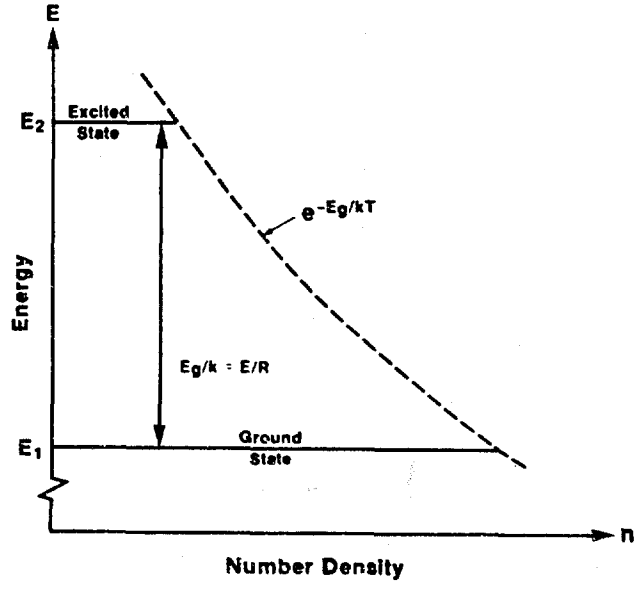


Fig. 3 - Energy Level Diagram for Excited and Ground State Fuel Molecules

The energy gap $E_g$ between these two states is such that

$$E_g/k = E/R \tag{1}$$

where E is the activation energy of the fuel, R is the Universal Gas Constant, and k is Boltzmann's Constant.

For this simple two-level model, rate equations describing transitions between the two states can be written as

$$\frac{dn_1}{dt} = -w_{12}\, n_1 + w_{21}\, n_2 \tag{2}$$

$$\frac{dn_2}{dt} = w_{12}\, n_1 - w_{21}\, n_2 - wn_2 \tag{3}$$

where $n_i$ is the density of molecules in state i, $w_{ij}$ is the transition rate from state i to state j, and the subscripts 1 and 2 refer to the ground and excited states, respectively. These equations are the same as for any two-level system (7), except for the final term of Equation 3: this term allows reaction of the excited molecules with oxygen, and states that the rate of such reactions is proportional to the density of excited molecules, $n_2$. Presumably, w itself would depend on the oxygen concentration, since in the absence of oxygen, no reactions would occur.

The heat given up to the surroundings as the excited molecules react with oxygen is given by

$$\frac{dT_s}{dt} = K\, wn_2 \tag{4}$$

where $T_s$ is the temperature of the surroundings, and K is the temperature rise which results when one fuel molecule reacts with oxygen.

Equations 2-4 can readily be extended to multi-level systems. Consider, for example, a system containing M energy levels which are arbitrarily numbered in ascending order from the lowest to the highest energy level. If the first m states are assumed to be ground states, and the remaining states (numbered from m+1 to M, inclusively) are excited states, the set of equations corresponding to Equations 2-4 can be written as

$$\frac{dn_j}{dt} = -\sum_{i\neq j}^{M} w_{ji}\, n_j + \sum_{i\neq j}^{M} w_{ij}\, n_i \qquad \text{for } 1\leq j\leq m \tag{5}$$

$$\frac{dn_j}{dt} = -\sum_{i\neq j}^{M} w_{ji}\, n_j + \sum_{i\neq j}^{M} w_{ij}\, n_i - w_j\, n_j \qquad \text{for } m+1\leq j\leq M \tag{6}$$

$$\frac{dT_s}{dt} = \sum_{j=m+1}^{M} K_j\, w_j\, n_j \tag{7}$$

Returning to the simple two-level system, Equation 4 states that the rate of heat release is directly proportional to the number of molecules in the excited state. We can thus anticipate that if $n_2$ is somehow increased prior to the fuel being exposed to oxygen, the observed ignition delay should be decreased. According to this model, this can be achieved simply by increasing the fuel temperature prior to exposing it to oxygen. To show this, assume that fuel is in thermal equilibrium with itself at temperature T and that no oxygen is present. Then w = 0, and the densities of states 1 and 2 are constant:

$$\frac{dn_1}{dt} = \frac{dn_2}{dt} = 0 = -w_{12}\, n_1 + w_{21}\, n_2 \tag{8}$$

Assuming Boltzmann statistics apply,

$$\frac{n_2}{n_1} = \frac{w_{12}}{w_{21}} = e^{-E_g/kT} = e^{-E/RT} \tag{9}$$

At room temperature, assuming an activation energy of 30 Kcal/mole,

$$\frac{n_2}{n_1} \approx 10^{-22} \tag{10}$$

For the same fuel at $10^3$°K, however,

$$\frac{n_2}{n_1} \approx 3 \times 10^{-7} \tag{11}$$

Referring to Equation 4, we can anticipate significant differences in the ignition delay for these two fuels.

## THEORETICAL RESULTS

The formal solution to Equations 2-4 will next be derived, subject to the following boundary conditions:

1. at $t = 0$, $n_1 + n_2 = N_o$
2. at $t = 0$, $n_2/n_1 = e^{-E/RT_f}$, where $T_f$ is the fuel temperature prior to injection.
3. at $t = 0$, $T_s = T_a$, where $T_a$ is the air temperature prior to injection.

The results are

$$\frac{n_1}{N_o} = \frac{1}{D}\left[-\left(1 - \frac{w}{s_+}\right) Ae^{-s_+ t} + \left(1 - \frac{s_-}{w}\right) Be^{-s_- t}\right] \tag{12}$$

$$\frac{n_2}{N_o} = \frac{1}{D}\left(Ae^{-s_+ t} + \frac{s_-}{w}\, Be^{-s_- t}\right) \tag{13}$$

$$\frac{dT_s}{dt} = K\, wn_2 \tag{14}$$

where

$$s_{\pm} = \frac{1}{2}\left((w_{12} + w_{21} + w) \pm \left[(w_{12} + w_{21} + w)^2 - 4ww_{12}\right]^{\frac{1}{2}}\right) \quad (15)$$

$$A = \left(1 - \frac{s_-}{w}\right) e^{-E/RT_f} - \frac{s_-}{w} \quad (16)$$

$$B = \left(1 - \frac{w}{s_+}\right) e^{-E/RT_f} + 1 \quad (17)$$

$$D = \left(1 - \frac{s_-}{s_+}\right)\left(1 + e^{-E/RT_f}\right) \quad (18)$$

APPROXIMATE SOLUTION - If it is assumed that

$$w << w_{12} + w_{21} \quad (19)$$

considerable simplification results since in this limit, $T_f$ approaches $T_s$ as t approaches infinity. Under these assumptions, Equations 13-18 can be simplified and combined to give

$$\frac{dT_s}{dt} \simeq KwN_o \left[e^{-E/RT_s}\left(1 - e^{-t/t_1}\right) + e^{-E/RT_f} e^{-t/t_1}\right] \quad (20)$$

where $t_1$ is a time constant given by

$$t_1 = (w_{12} + w_{21})^{-1} \quad (21)$$

and can be expected to be different for various fuels. This approximate solution will next be applied to four cases in order to better understand results which will be shown later for the complete solution.

Case 1 - At t = 0, assume $T_f = T_s = T_a$ (premixed fuel and air). From Equation 20,

$$\frac{dT_s}{dt} \simeq KwN_o e^{-E/RT_s} \quad (22)$$

Integration of this equation leads to

$$\int_0^{\tau} dt \simeq \frac{1}{KwN_o} \int_{T_a}^{T_{ig}} e^{+E/RT_s} dT_s \quad (23)$$

where the ignition delay, $\tau$, has been defined as that time at which $T_s = T_{ig}$, the ignition temperature.

Assuming $T_a$ is negligible in comparison to $T_{ig}$ leads to

$$\tau \simeq \frac{1}{KwN_o} e^{E/RT_a} \quad (24)$$

This predicts what has been observed experimentally (8), namely that the ignition delay is inversely proportional to oxygen concentration and pressure ($wN_o$), and displays an exponential dependence on reciprocal temperature.

Case 2 - At t = 0, $T_f << T_a << T_{ig}$ (cold fuel injected into warm air).

In this case, the last term of Equation 20 is negligible for $t \lesssim t_1$, and it is presumed that ignition occurs after $t_1$, again leading to Equation 22 et. seq. Thus, in this case, cold fuel rapidly equilibrates with the air and leads to an ignition delay which is the same as it would have been with premixed fuel and air.

Case 3 - At t = 0, $T_f << T_a < T_{ig}$ (cold fuel injected into hot air).

Again, the last term of Equation 20 is negligible, but it is now assumed that $e^{-E/RT_s}$ has so large a valve that the thermal transient cannot be overlooked. Expanding the first term of Equation 20 about t = 0 gives

$$\frac{dT_s}{dt} \simeq KwN_o \, t/t_1 \, e^{-E/RT_s} \quad (25)$$

which lead to

$$\tau \simeq e^{E/2RT_a} \quad (26)$$

As will be seen, this is not exactly as observed experimentally, but it demonstrates the correct behavior, namely, as the air temperature is increased, the observed ignition delay is less sensitive to air temperature.

Case 4 - At t = 0, $T_f >> T_a$ (hot fuel injected into air). Here the last term of Equation 20 is assumed to dominate, and it is presumed that ignition will occur within a time interval shorter than $t_1$. Thus,

$$\frac{dT_s}{dt} \simeq KwN_o e^{-E/RT_f} \quad (27)$$

or,

$$\tau \simeq \frac{1}{KwN_o} e^{E/RT_f} \quad (28)$$

This result predicts that the ignition delay can be made arbitrarily small if the initial oxygen concentration and fuel temperature are sufficiently high. Furthermore, it predicts that in this limit, the ignition delay will be independent of air temperature.

RESULTS FOR CETANE - In an attempt to see how well this model predicts ignition delay, values of the constants were picked which gave good agreement between theoretical and experimental results (9) for room temperature cetane injected into air. As shown in Figure 4 for $T_f \leq 500°K$, agreement between theoretical and experimental results is remarkably good, considering such a simple model for fuel. Note the discrepancy is worse at extremely high air temperature, suggesting that temperature dependent values of the constants should be

considered, or, that more than two levels should be considered. Notice also that the curvature of ln $\tau$ versus $1/T_a$ is different for $T_f \geq 700°K$ than it is for $T_f \leq 600°K$, in general agreement with published data (3).

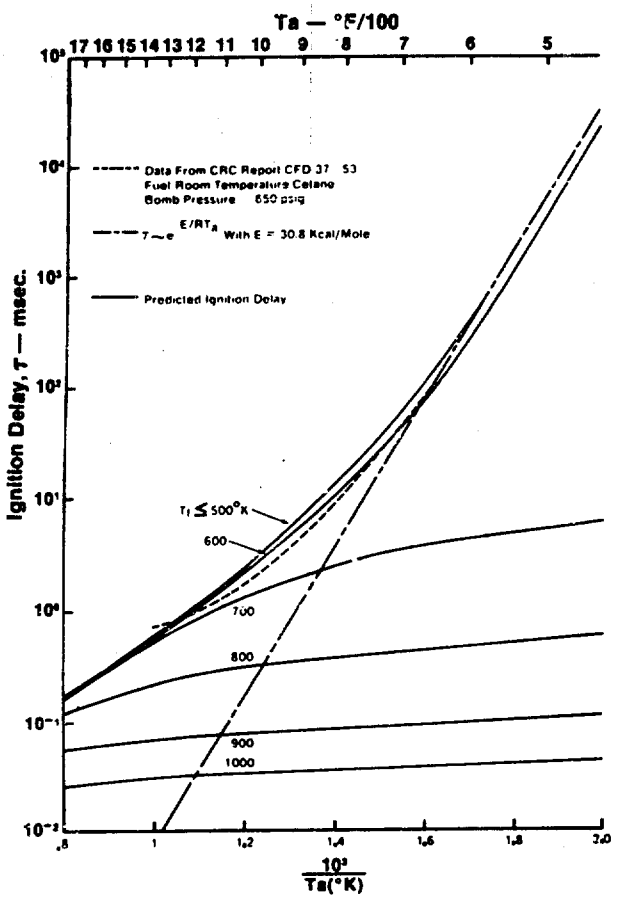


Fig. 4 - Experimental and Theoretical Ignition Delay Versus Reciprocal Air Temperature for Various Initial Fuel Temperatures

## CONCLUSIONS

The new model predicts many of the trends in ignition delay which have been observed. A simple two-level model shows remarkable agreement with published data for room temperature cetane injected into air. Conceivably, a multi-level solution would predict multi-stage ignition or cool flame phenomena which have been observed.

## REFERENCES


1. Gerrish, H. C. and Ayer, B. E., "Influence of Fuel-Oil Temperature on the Combustion in a Prechamber Compression Ignition Engine," NACA TN565, 1936.

2. Holmes, V. V. et al., "Combustion of a Low Volatility Fuel in a Turbojet Combustion Chamber-Effects of Fuel Vaporization," TRANS ASME 75, pp. 1303-1310.

3. Spadaccini, L. J., "Autoignition Characteristics of Hydrocarbon Fuels at Elevated Temperatures and Pressures," ASME Paper No. 76-GT-3, 1976.

4. DeZubay, E. A., "A Note on the Autoignition of Liquid Fuels," Combust. Flame 32, 313-315 (1978).

5. Messiah, A., Quantum Mechanics, North-Holland Published Co., 1966.

6. Halstead, M. P., et al., "The Autoignition of Hydrocarbon Fuels at High Temperatures and Pressures," Comubst. Flame 30, 45-60 (1977).

7. Siegman, A. E., Microwave Solid-State Masers, McGraw-Hill, 1974, pp. 153-158.

8. Mullins, B. P., "Studies on the Spontaneous Ignition of Fuels Injected into a Hot Air Stream," Parts I-VIII, Fuel 31 and 32, 1952 and 1953.

9. "Combustion Characteristics-Ignition Delay Bomb," Coordinating Research Council Report 297, 1955.

## DISTRIBUTION LIST

| | Copies |
|---|---|
| U. S. Army TACOM<br>Attn: DRSTA-RG<br>Warren, MI 48090 | 10 |
| Commander<br>U. S. Army TACOM<br>Attn: DRSTA-TSL<br>Warren, MI 48090 | 2 |
| Defense Technical Information Center<br>Cameron Station<br>5010 Duke Street<br>Alexandria, VA 22314 | 15 |
| Manager<br>Defense Logistics Studies<br>Information Exchange<br>ATTN: DRXMC-D<br>Fort Lee, VA 23801 | 2 |